Conductivity of Select Materials

Substance	σ (S/m)	*Substance*	σ (S/m)
Ag	6.2×10^7	$Bi_2Ru_2O_7$	2×10^5
Cu	5.9×10^7	$LaNiO_3$	1×10^5
Al	3.8×10^7	doped polyacetylene	8×10^4
Na	2.1×10^7	Fe_3O_4	2×10^4
ReO_3	1.1×10^7	$YBa_2Cu_3O_7$*	1×10^2
Ti	2.5×10^6	Ge	2×10^0
La	1.6×10^6	Si	10^{-3}
$SrMoO_3$	1.0×10^6	NiO	10^{-8}
Bi	7.7×10^5	Al_2O_3	10^{-12}
Mn	6.2×10^5	S	10^{-15}
NbN	4×10^5	SiO_2 (Quartz)	10^{-16}
TiO	3×10^5	Teflon	10^{-22}

Organic Conductors

From Polymers to Nanotubes

Structure, Bonding & Electronic Properties

Chapter 10.5 - 10.6

Learning Objectives

- Explain how π-conjugation leads to delocalized molecular orbitals that form bands
- Relate Peierls distortion and redox doping to the band gap and carrier formation in polymers
- Define nanotube (n,m) indices and compute diameter and chiral angle
- Predict metallic vs semiconducting behavior from the $(n-m)/3$ rule and $E_g \propto 1/d$
- Compare transport limits in polymers vs nanotubes and link back to structure

Why Organic Conductors?

Breaking the Paradigm

- Traditional view: organics = insulators
- 1970s revolution: conjugated systems conduct
- Conductivity spans 15 orders of magnitude
- 2000 Nobel Prize in Chemistry

Key Advantages

- **Lightweight** & flexible
- **Solution processable**
- **Tunable** properties
- **Applications:** OLEDs, solar cells, sensors

Application Area	Estimated Market Size (USD)	Notes
OLED / Organic Electronics (displays, flexible devices)	**~46 B**	By far the largest real-world use of organic conductors; includes OLED materials and organic layers in display stacks.
Conductive Polymers (coatings, EMI shielding, antistatic, electronics)	**~5 B**	Pure organic conductor materials used in coatings, components, printed electronics interfaces.
Organic Photovoltaics / Polymer Solar Cells	**~1.7 B**	Rapid growth; still small compared with displays but expanding quickly.
Sensors, Actuators, Printed Electronics	**~0.8 B**	Includes wearables, IoT devices, smart materials using organic conductors.
Bioelectronics / Medical & Wearable Interfaces	**0.1–1 B** (varies)	Highly specialized; smaller but high-value and growing.

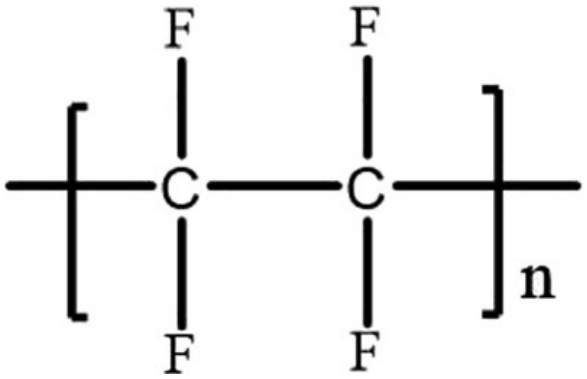

Teflon

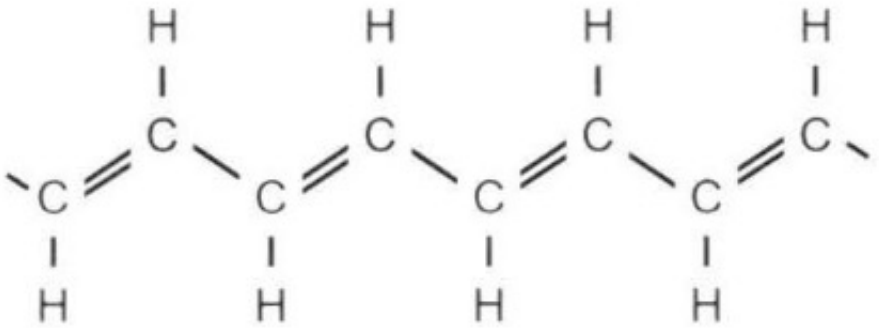

trans-polyacetylene

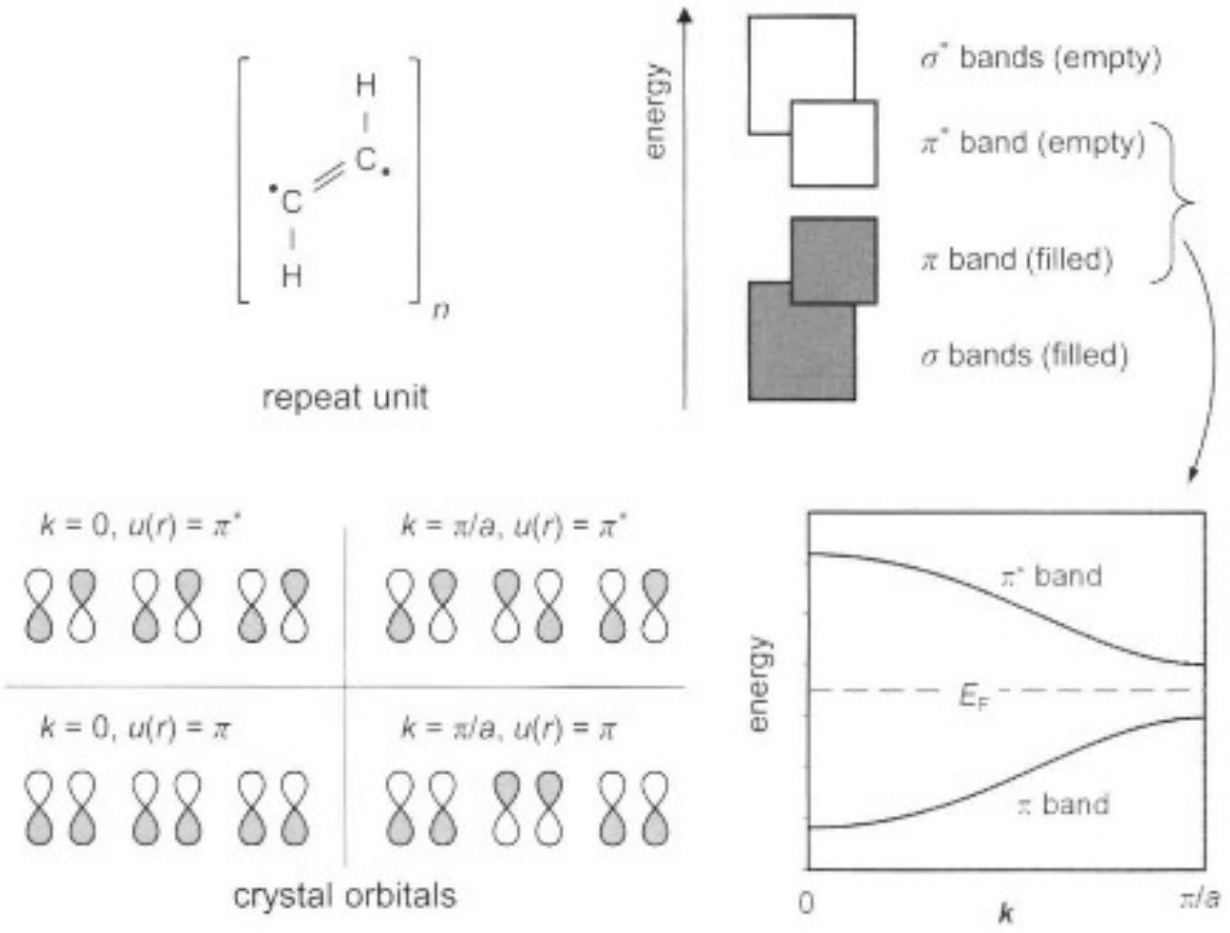
H
C
C
H
n
repeat unit
energy
σ* bands (empty)
π* band (empty)
π band (filled)
σ bands (filled)
k = 0, u(r) = π*
k = π/a, u(r) = π*
k = 0, u(r) = π
k = π/a, u(r) = π
crystal orbitals
energy
π* band
E_F
π band
0
k
π/a

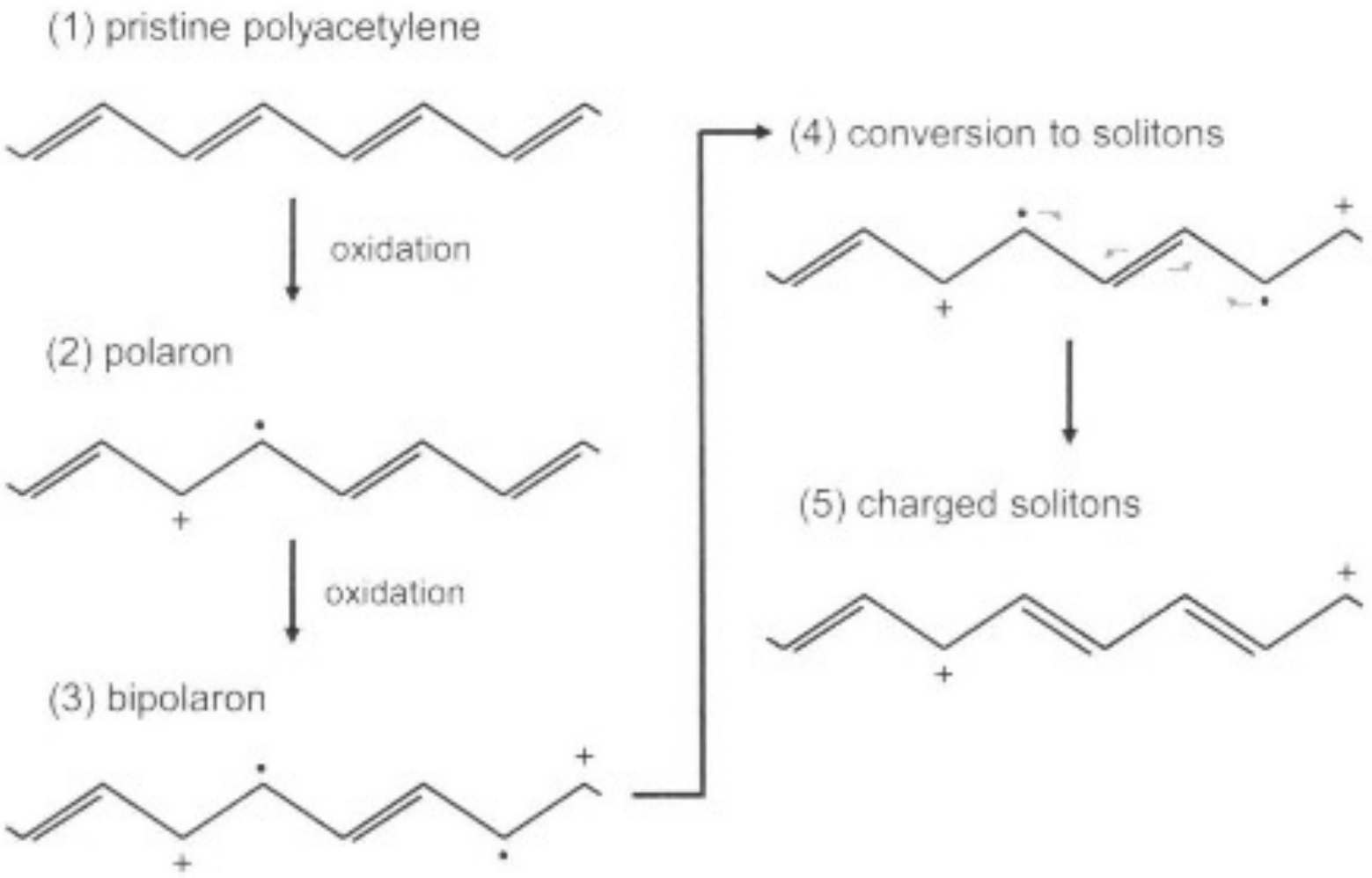
(1) pristine polyacetylene
oxidation
(2) polaron
oxidation
(3) bipolaron
(4) conversion to solitons
(5) charged solitons

The Polymer

PEDOT:PSS = poly(3,4-ethylenedioxythiophene):polystyrene sulfonate

A complex of:

PEDOT

Conducting polymer backbone

PSS

Polyanion for water dispersibility

This unique combination enables commercial success

PEDOT

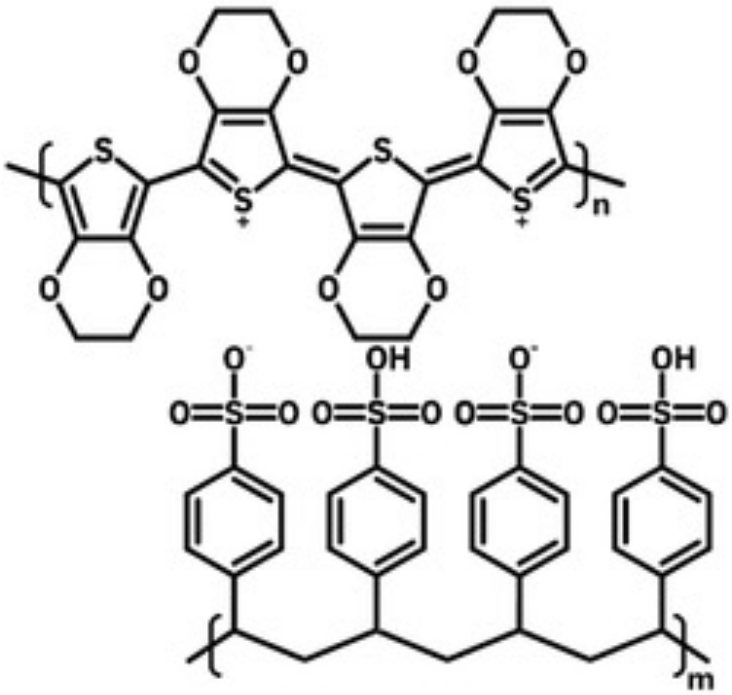

PSS

Key Advantage #1: Water Processable

The single biggest reason for commercial success

Processing Methods

- Solution casting at room temperature
- Spin coating
- Screen printing
- Roll-to-roll compatible
- Standard coating tools

Competitive Advantage

Other conducting polymers require:

- Harsh organic solvents
- In-situ oxidative polymerization
- Special handling conditions

Key Advantages #2 & #3: Stability & Film Quality

#2 Air Stable

Unlike most conducting polymers that degrade in oxygen/moisture

- Storage without special precautions
- Standard shipping & handling
- Long shelf life

#3 Superior Films

Essential for electronics:

- Optically clear
- Uniform thickness
- Low surface roughness
- No cracking or defects

Key Advantages #4 & #5: Tunability & Industry Fit

Tunable Conductivity

Adjust PEDOT:PSS ratio or add dopants:

1 S/cm → 1000+ S/cm

Secondary dopants: DMSO, ethylene glycol, sorbitol

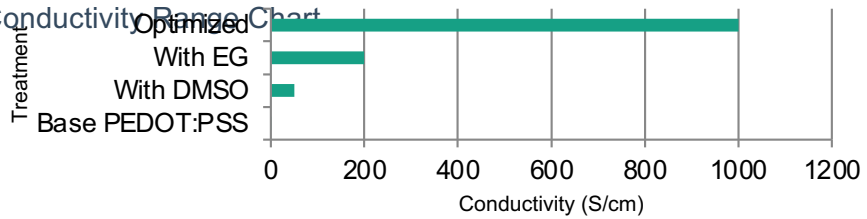

Industry Compatible

Direct integration into:

- OLED displays
- Touch panels
- Photovoltaics
- Sensors
- Antistatic coatings

No exotic equipment needed

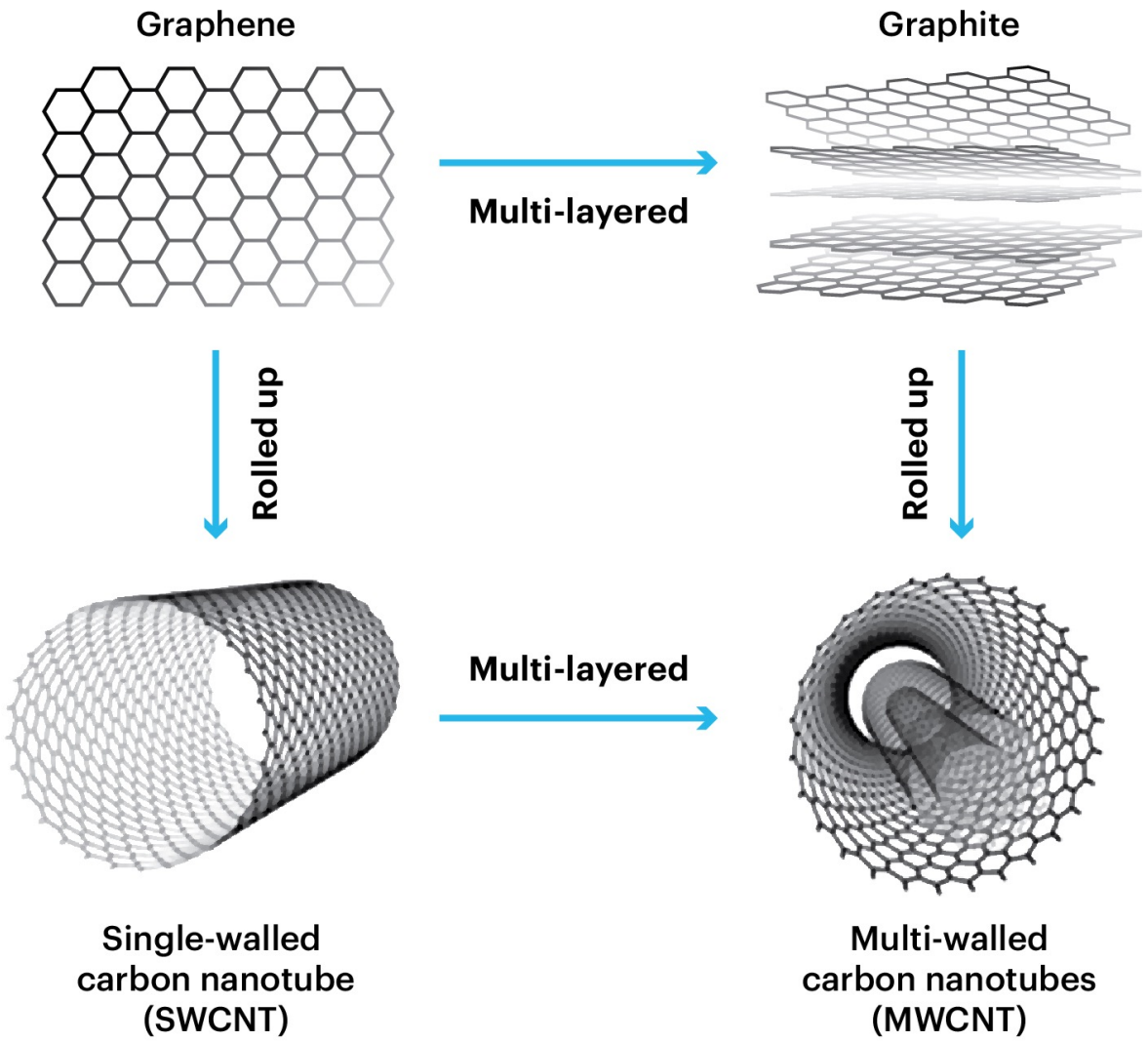
Graphene
Graphite
Multi-layered
Rolled up
Rolled up
Multi-layered
Single-walled
carbon nanotube
(SWCNT)
Multi-walled
carbon nanotubes
(MWCNT)

Hexagonal Lattice (Definition of Vectors)

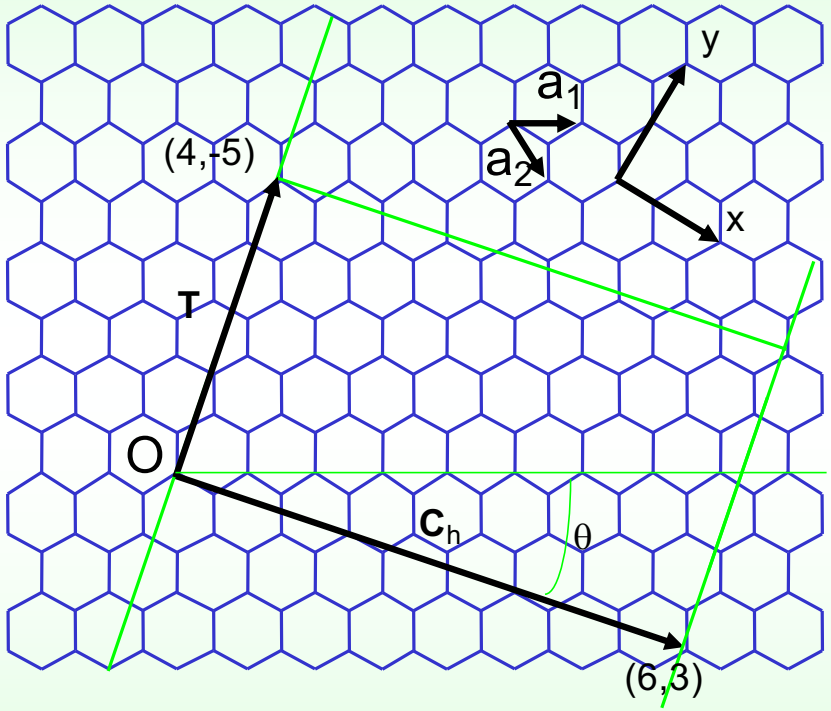

Chiral vector

$$\mathbf{C}_h = n\mathbf{a}_1 + m\mathbf{a}_2$$

$$\mathbf{a}_1 = (\frac{3}{2}a_{cc}, \frac{\sqrt{3}}{2}a_{cc})$$

$$\mathbf{a}_2 = (\frac{3}{2}a_{cc}, -\frac{\sqrt{3}}{2}a_{cc})$$

$$|\mathbf{a}_1| = |\mathbf{a}_2| = \sqrt{3}a_{cc} \equiv a$$

$$\mathbf{a}_1 = (\frac{\sqrt{3}}{2}, \frac{1}{2})a$$

$$\mathbf{a}_2 = (\frac{\sqrt{3}}{2}, -\frac{1}{2})a$$

Wrapping (10,0) SWNT (zigzag)

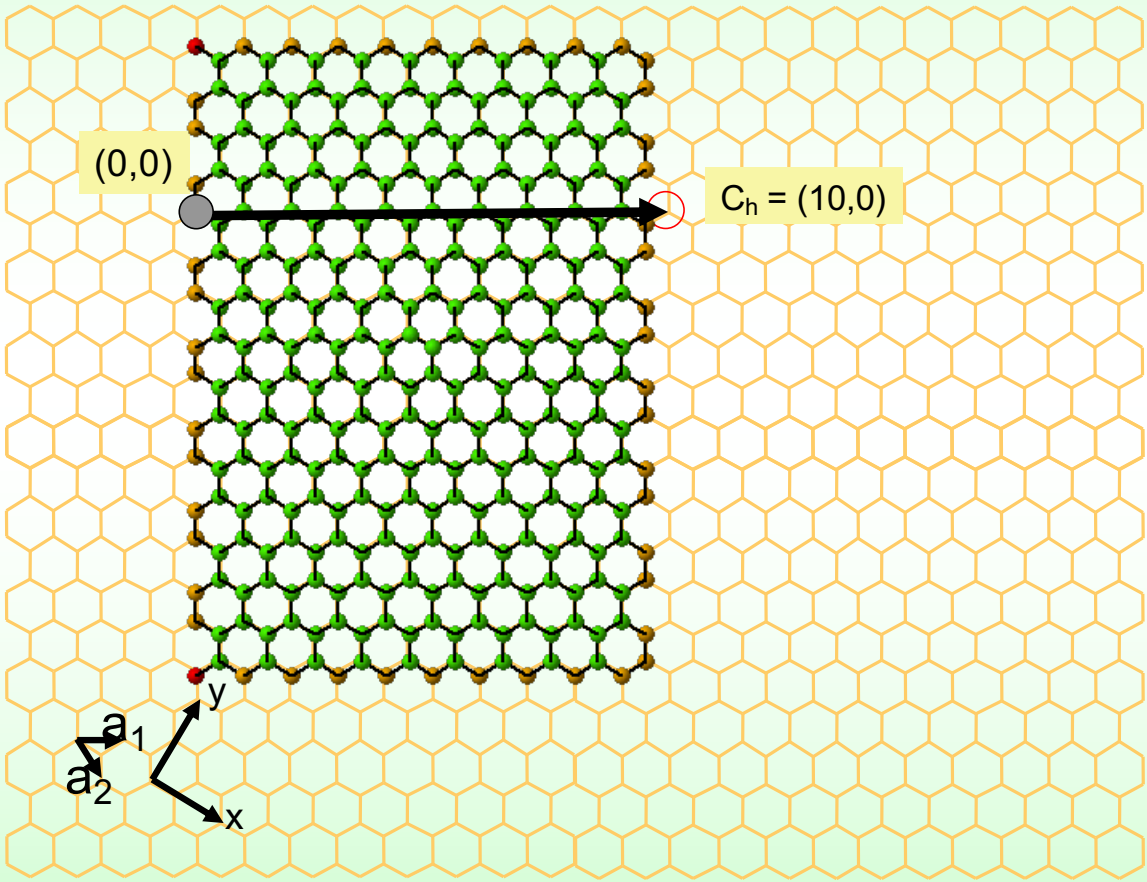

Wrapping (10,0) SWNT (Animation)

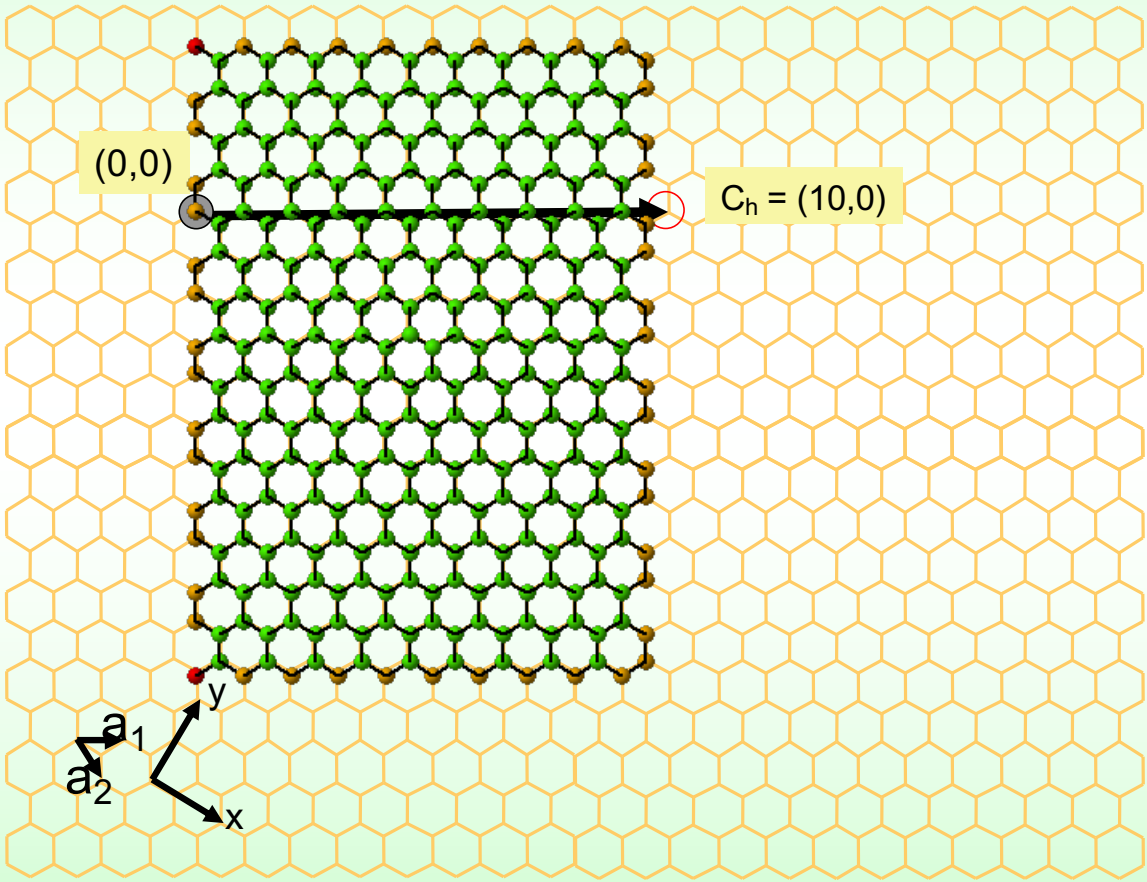

Wrapping (10,10) SWNT (armchair)

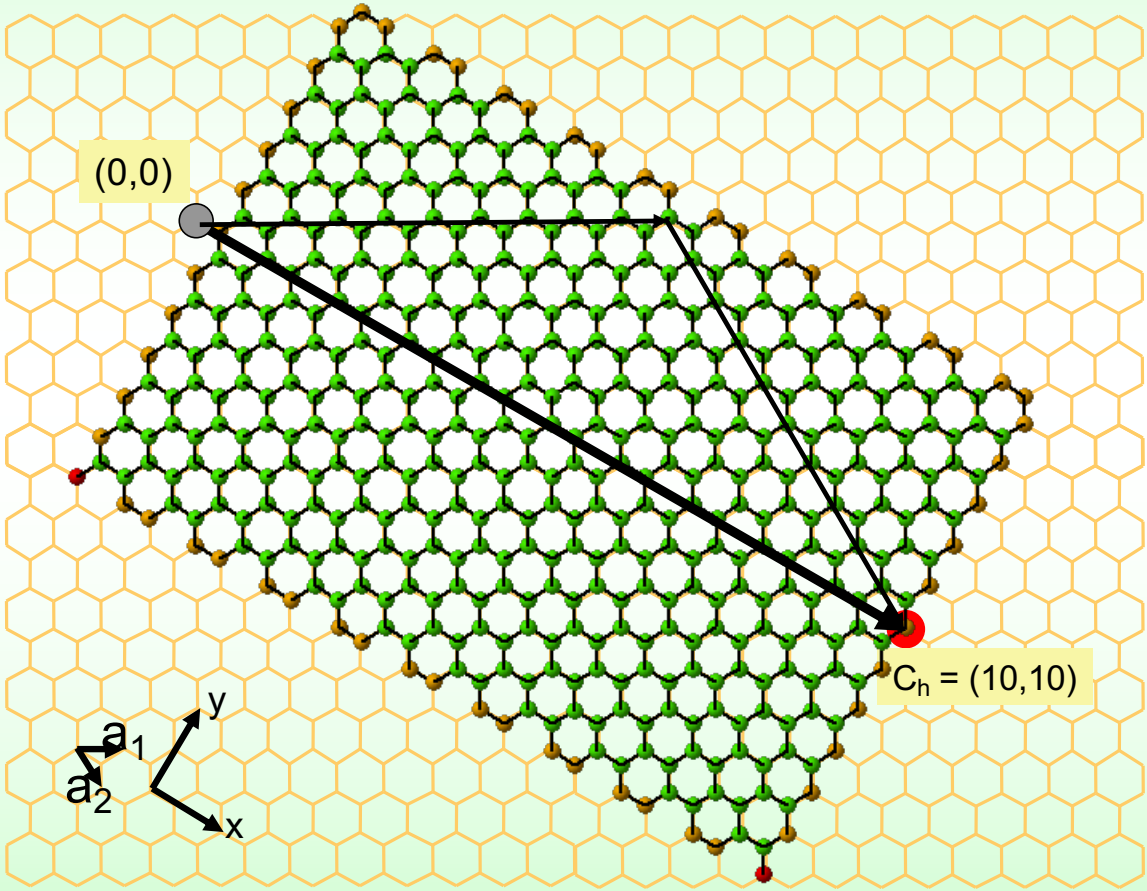

Wrapping (10,10) SWNT (Animation)

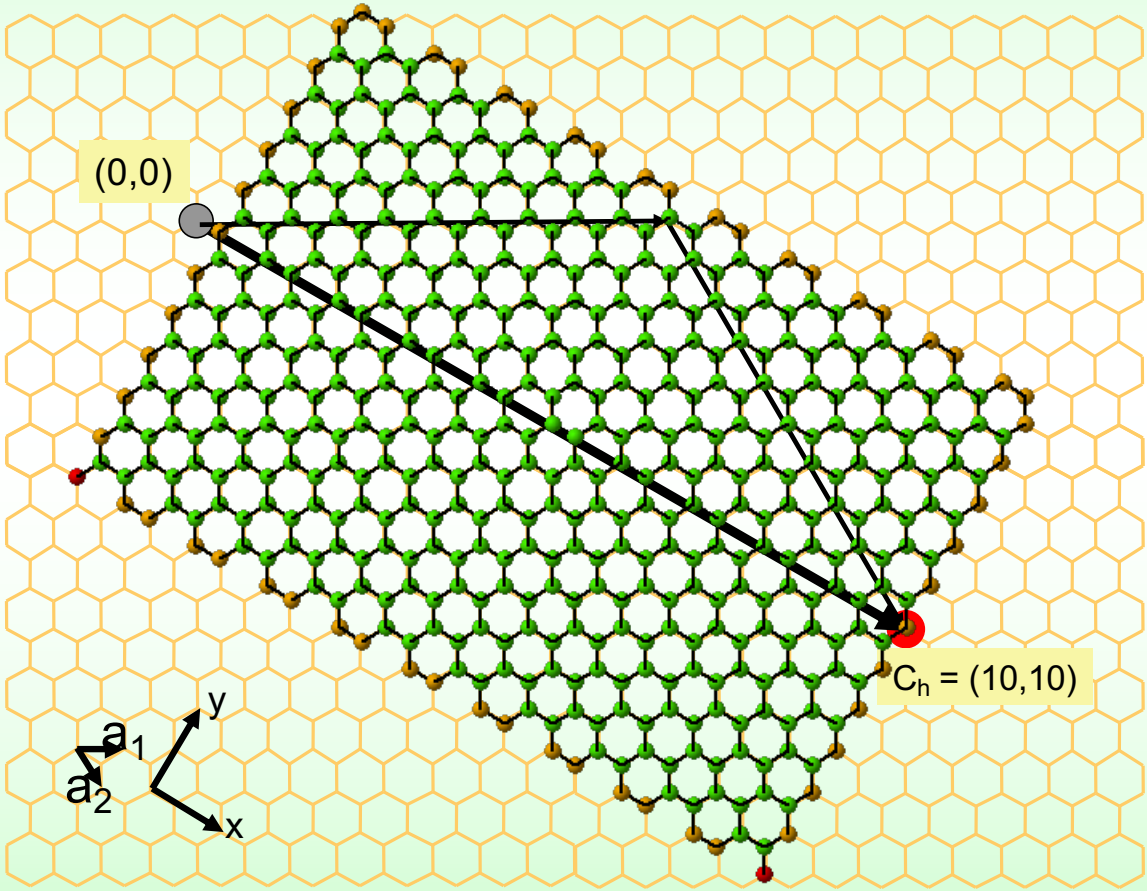

Wrapping (10,5) SWNT (chiral)

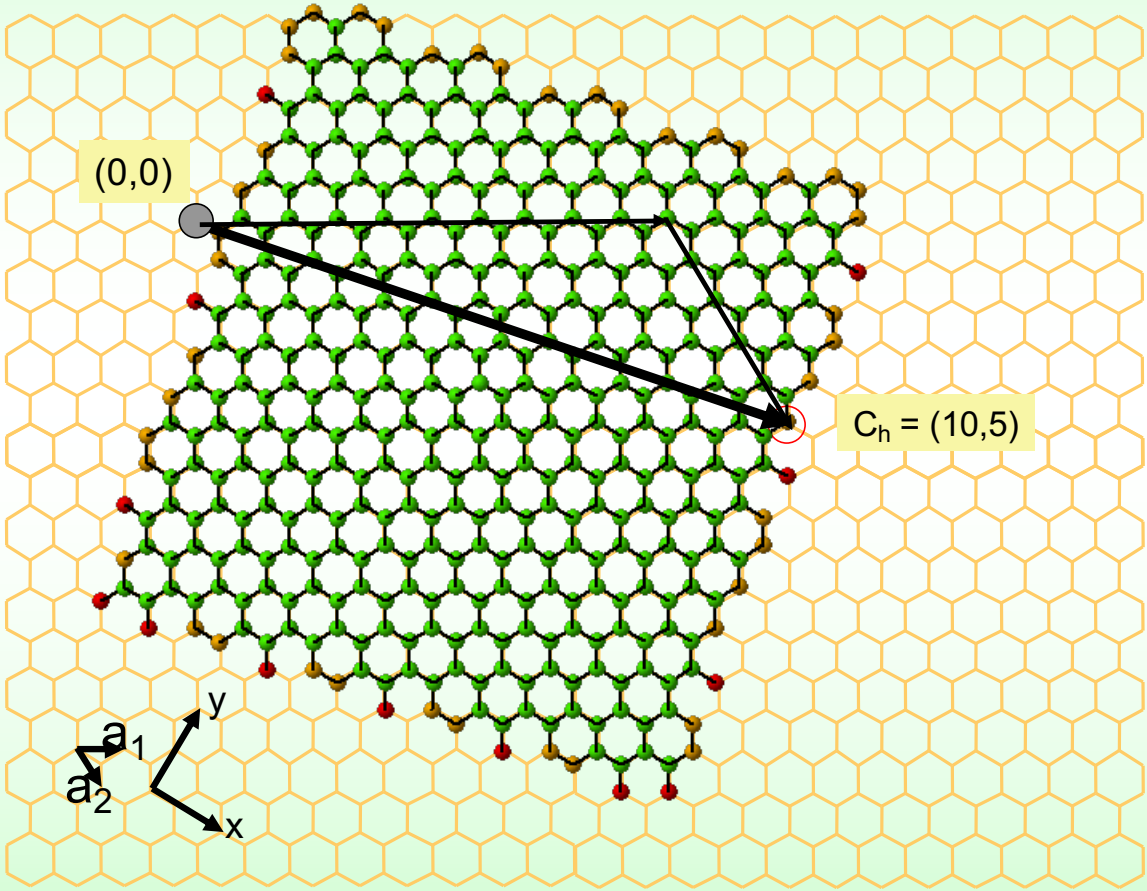

Wrapping (10,5) SWNT (Animation)

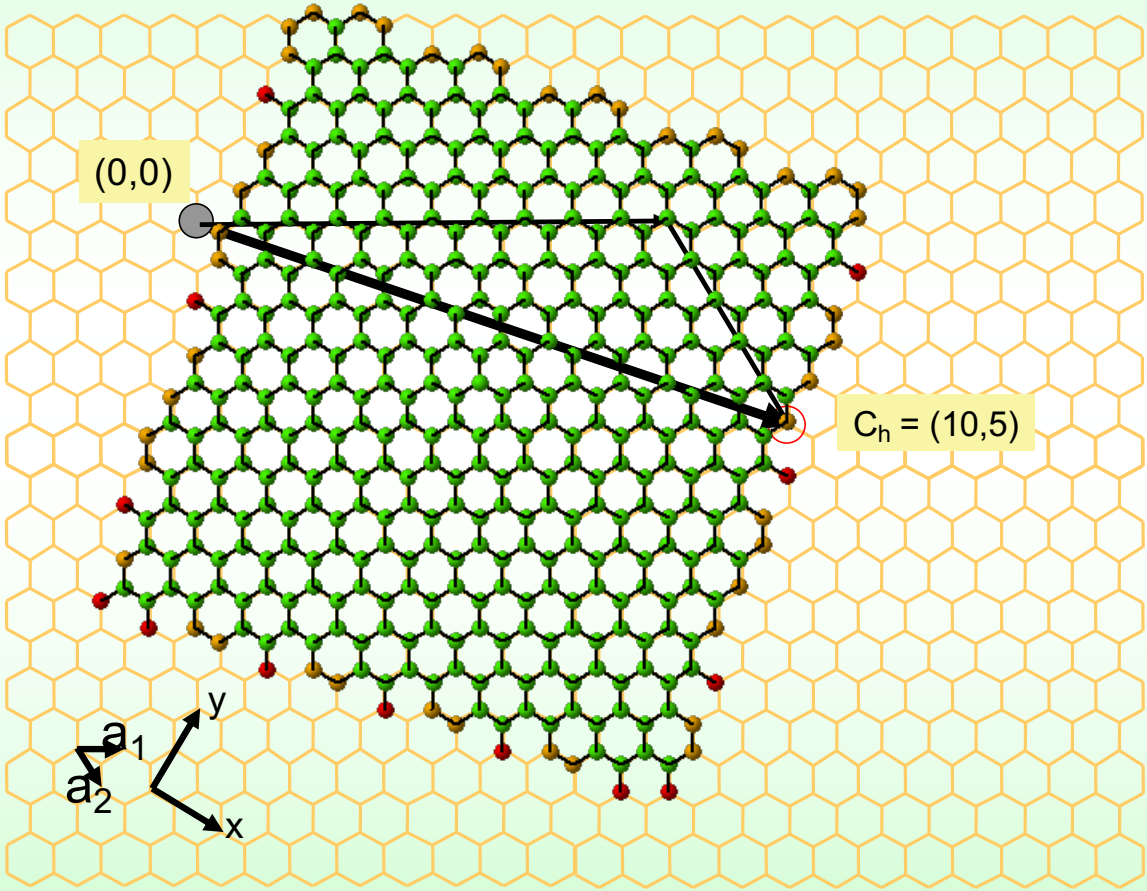

Hexagonal Lattice (n,m) nanotubes

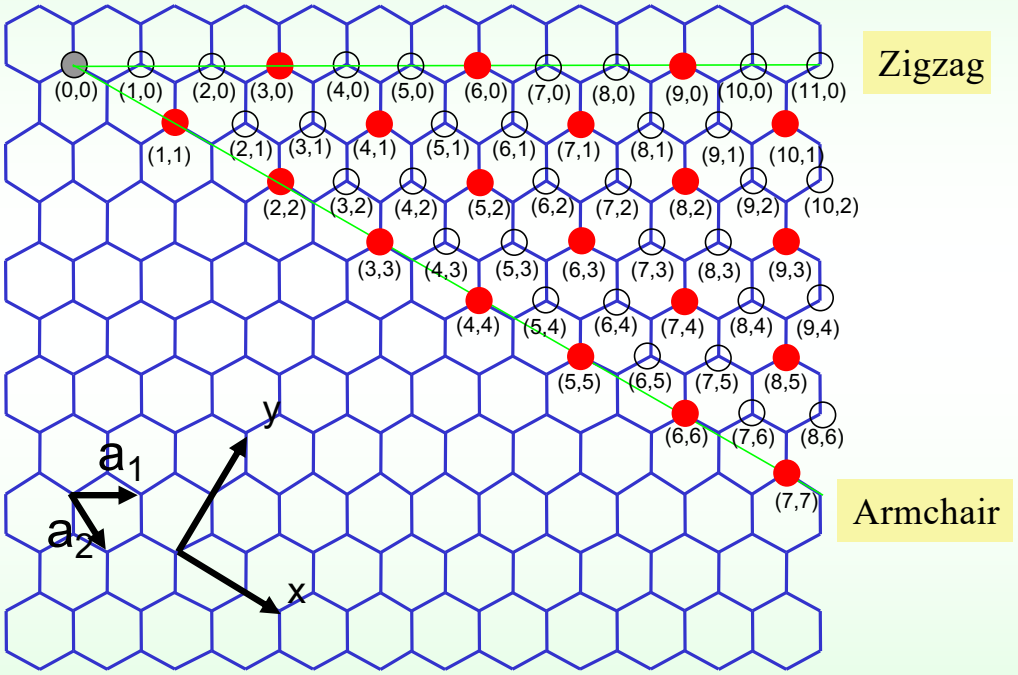

n - m = 3q (q: integer): metallic

n - m ≠ 3q (q: integer): semiconductor

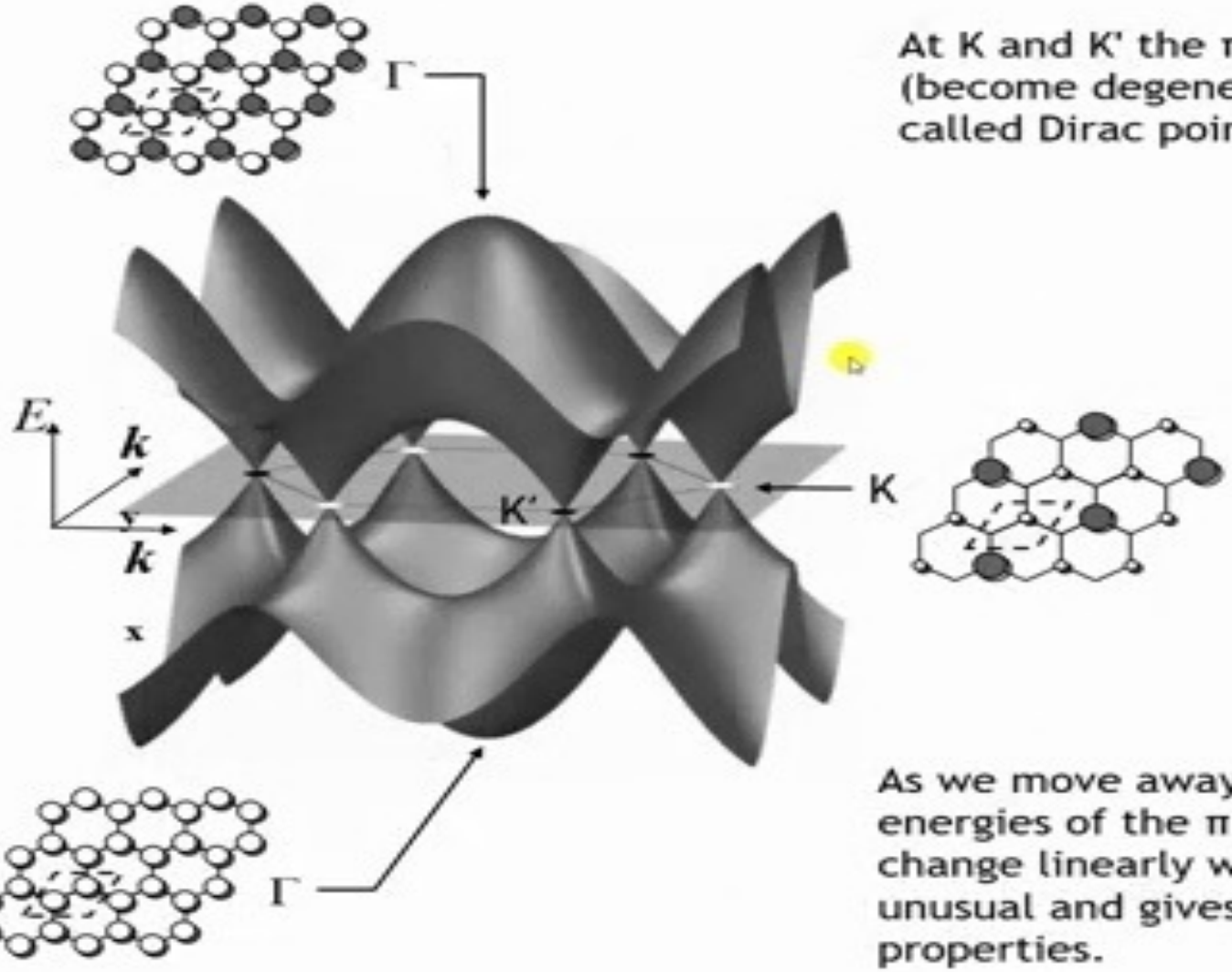

At K and K' the π and π* touch (become degenerate) these are called Dirac points

As we move away from K and K' the energies of the π and π* bands change linearly with ***k***. This is unusual and gives graphene special properties.

Why Some Nanotubes Are Metallic and Others Are Semiconducting

- **Rolling graphene into a nanotube imposes a periodic boundary condition** around the circumference defined by the chiral vector $\mathbf{C}_\mathrm{h} = n\mathbf{a}_1 + m\mathbf{a}_2$.

Metallic or
Semiconducting?

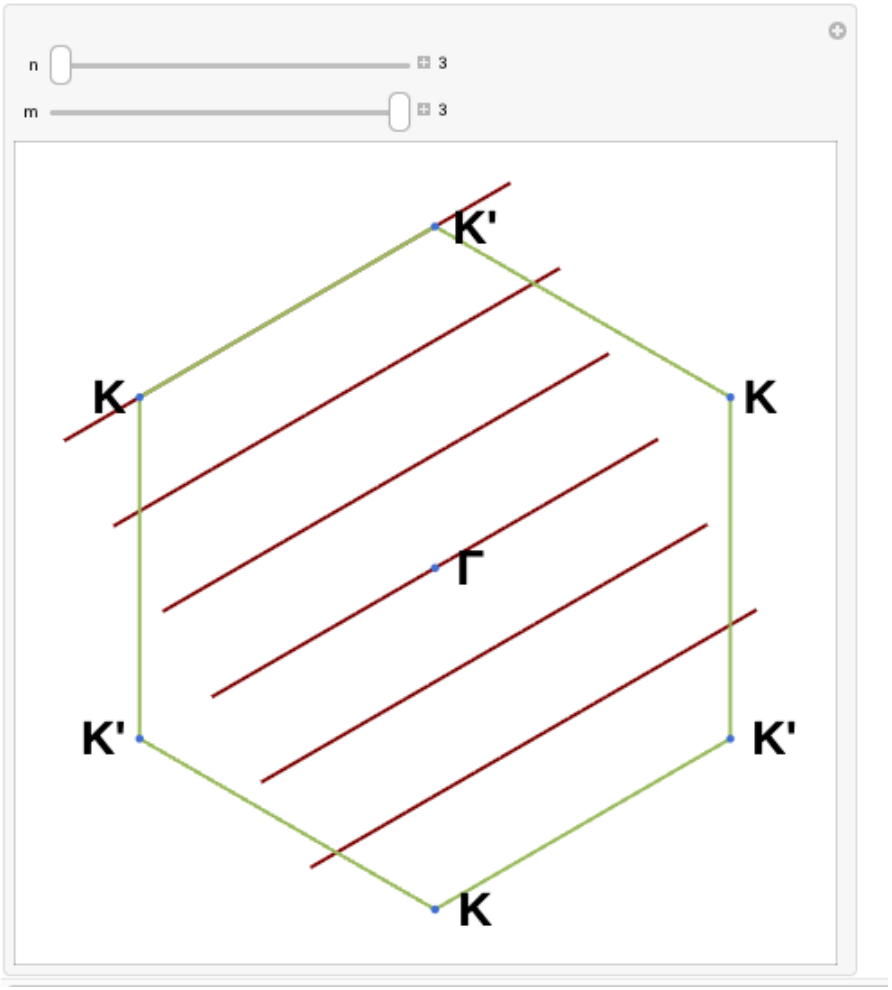

https://demonstrations.wolfram.com/BrillouinZoneOfASingleWalledCarbonNanotube/

Metallic or
Semiconducting?

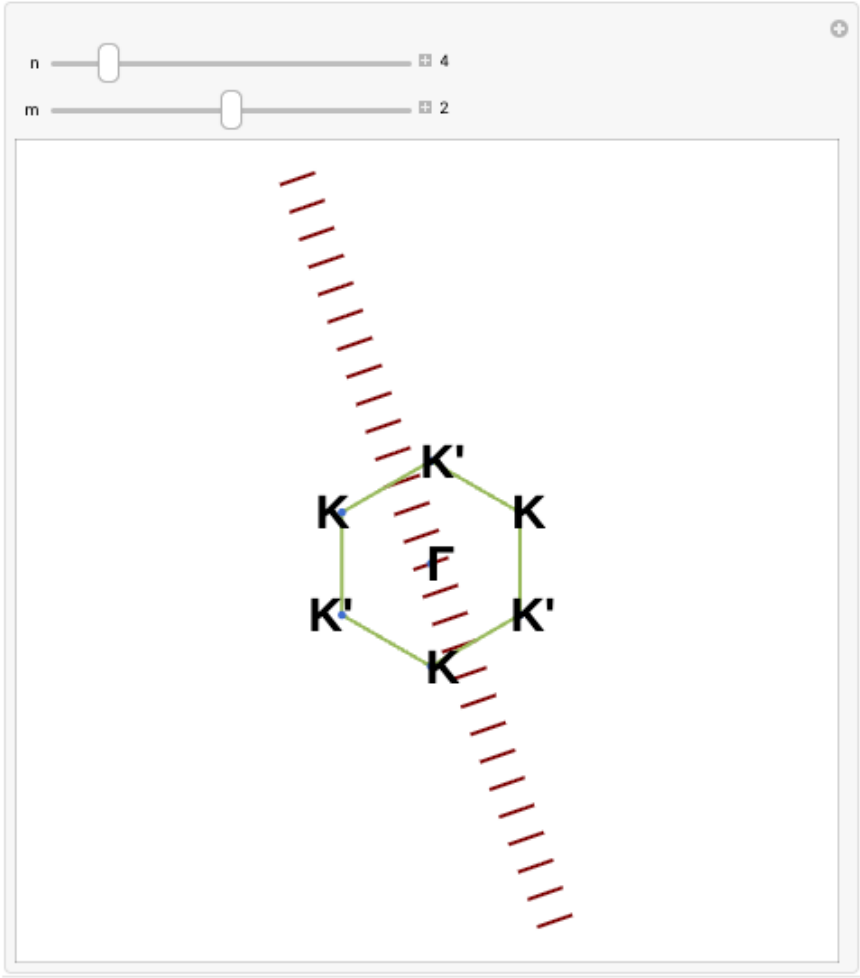

https://demonstrations.wolfram.com/BrillouinZoneOfASingleWalledCarbonNanotube/

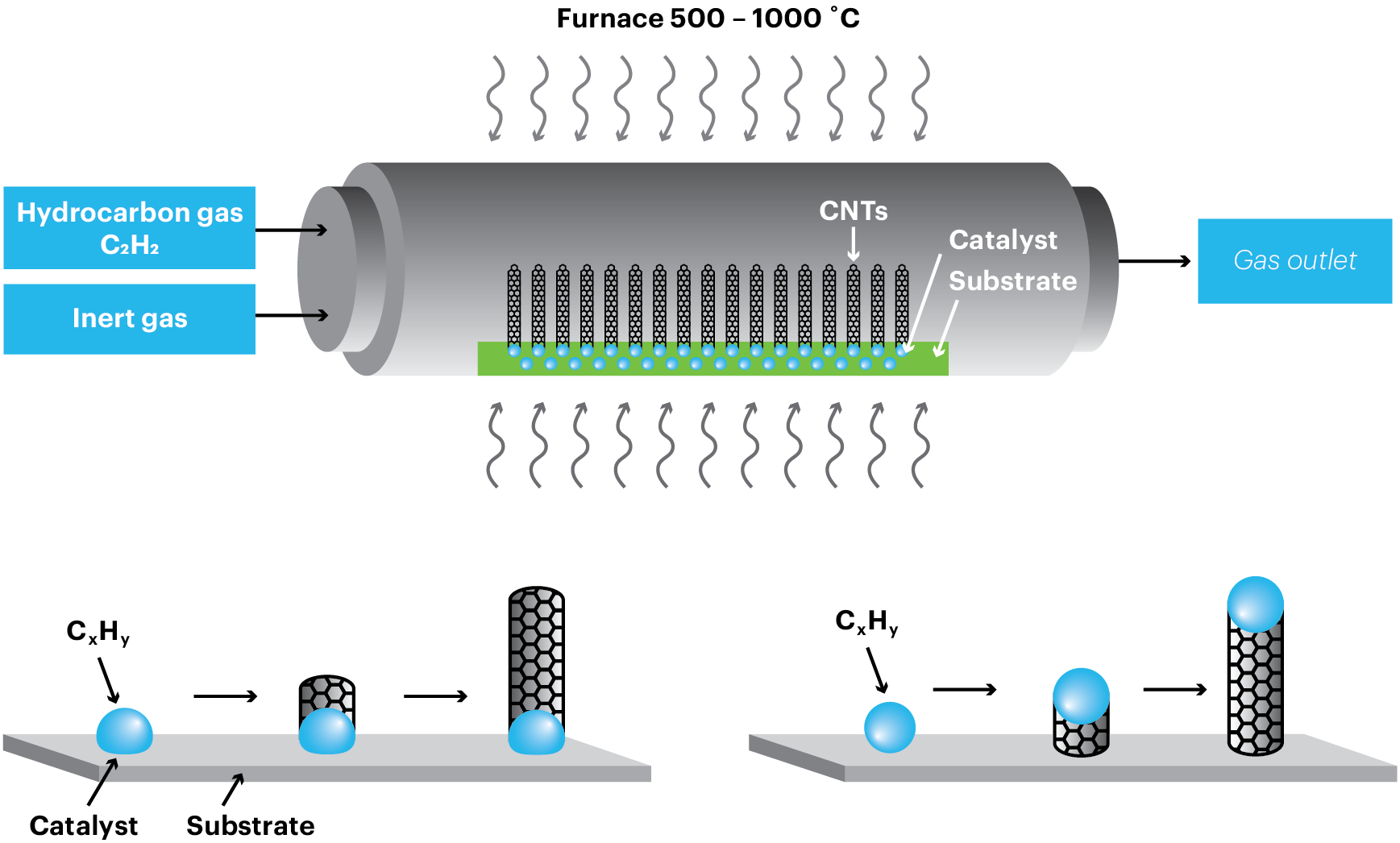

Figure 2. *Diagram of the standard chemical vapor deposition (CVD) method for synthesizing carbon nanotubes*

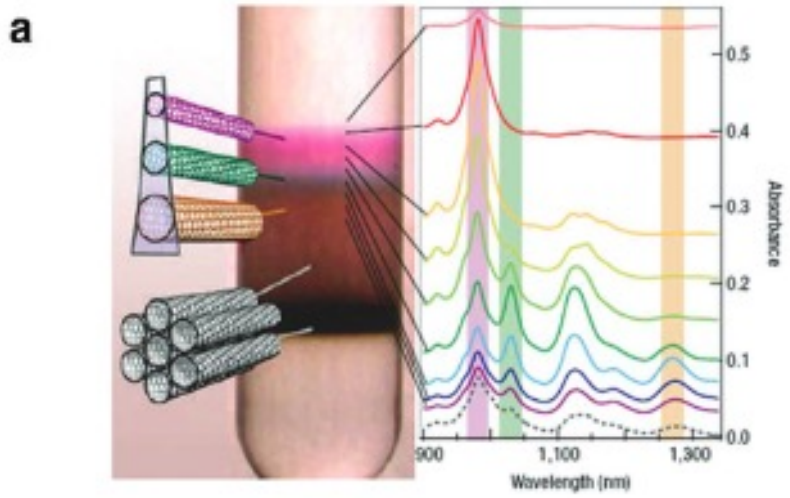

Ultracentrifuge Separation

M. S. Arnold, A. A. Green, J. F. Hulvat, S. I. Stupp, M. C. Hersam,Nat. Nanotechnol. 2006, 1, 60.

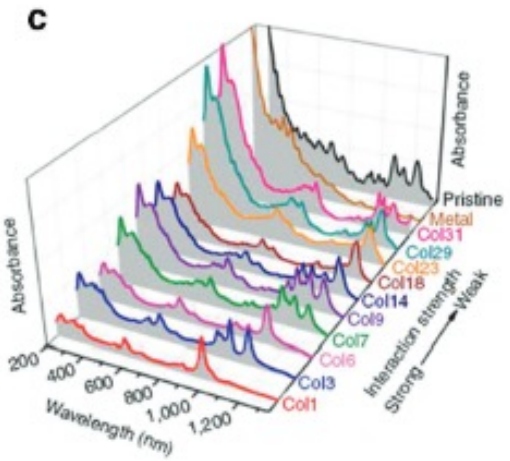

Chromatographic Separation

H. Liu, D. Nishide, T. Tanaka, H. Kataura, Nat. Commun. 2011, 2,309.

Application Area	Estimated Market Size (USD)	Notes
CNT-enhanced composites (plastics, automotive, aerospace, sports equipment)	**~1.2–1.5 B**	Largest current CNT use; small CNT loadings improve conductivity, strength, ESD resistance; used in automotive fuel systems, EV lightweighting, structural materials.
CNT conductive additives for Li-ion batteries	**~0.9–1.1 B**	Fastest-growing segment; CNTs used as conductive networks in battery cathodes/anodes; driven by EV growth; increasingly replacing carbon black in high-performance cells.
Transparent / conductive films & coatings	**~0.2–0.3 B**	Used in flexible displays, touch panels, heaters; CNT films compete with ITO in specialty applications where flexibility or durability is required.
Sensors and electronics (RF devices, nanosensors, interconnects)	**~0.1–0.2 B**	Includes strain sensors, biosensors, gas sensors, and early nanoelectronic components; small market but high R&D intensity.
CNT powders, inks, dispersions	**~0.1 B**	Base materials sold as powders, masterbatches, dispersions; sold to electronics, composites, and energy manufacturers.

Homework:

Conducting polymers: **10.17**

Carbon nanotubes: **10.18, 10.19, 10.20, 10.21, 10.22**

Chapter 12:
SUPERCONDUCTORS

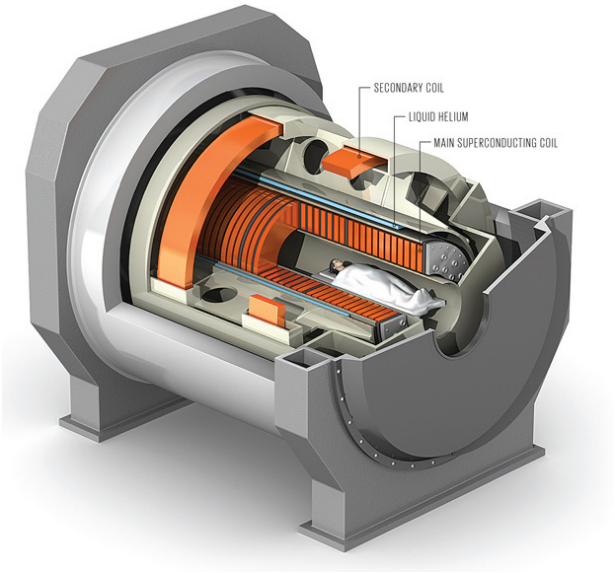

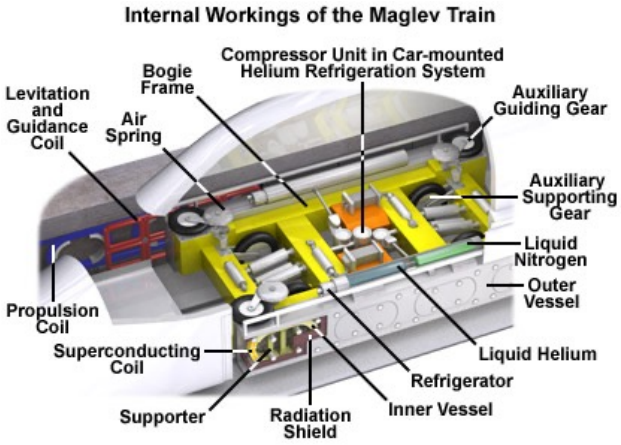

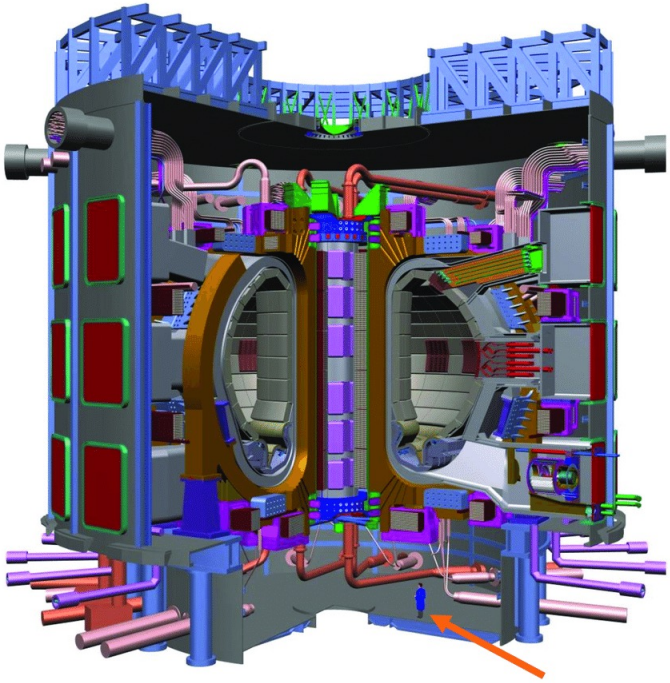

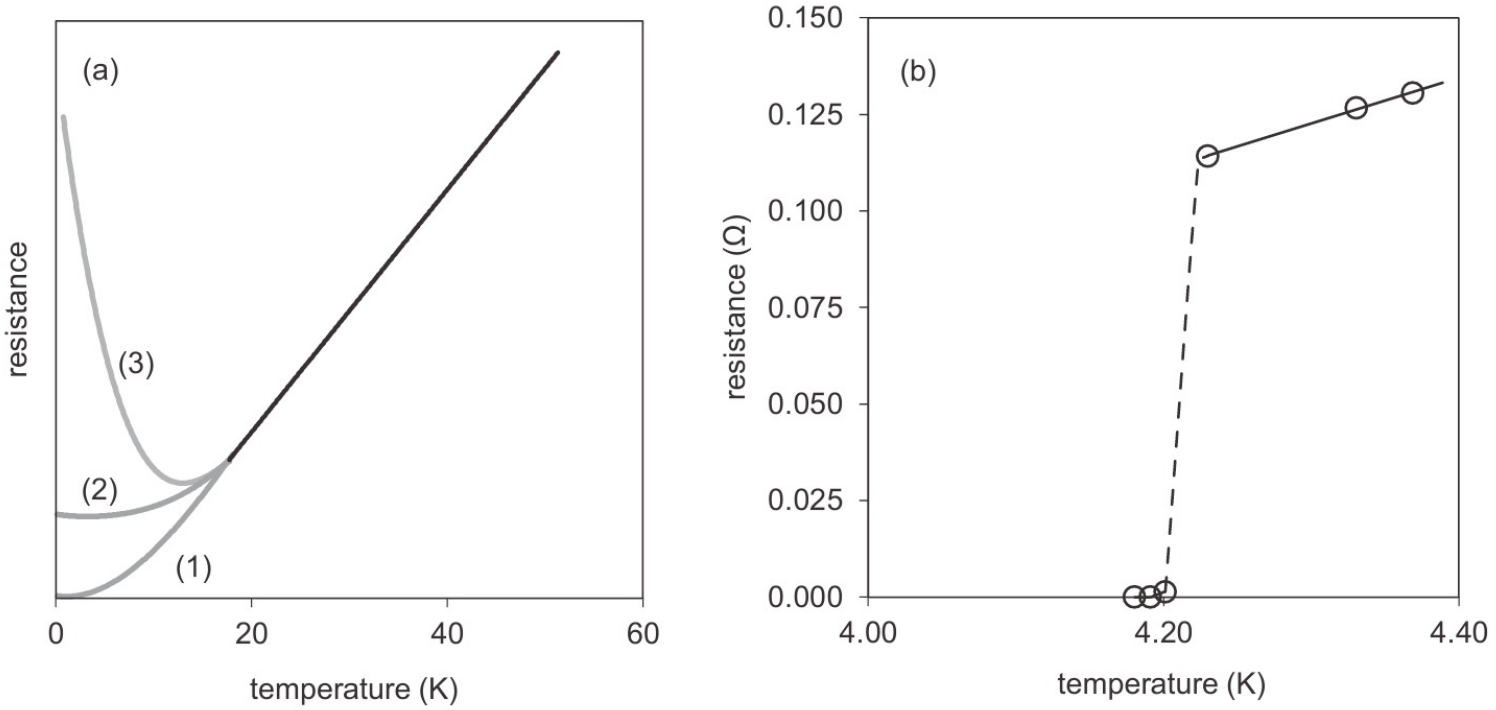

Figure 12.1 (a) Early postulated models for how a metal's resistance might vary with temperature as discussed in the text. (b) Onnes' original data on the resistance of Hg metal; below a critical temperature T_c of 4.2 K (the best modern value is 4.153 K), resistance falls to ~0 Ω.

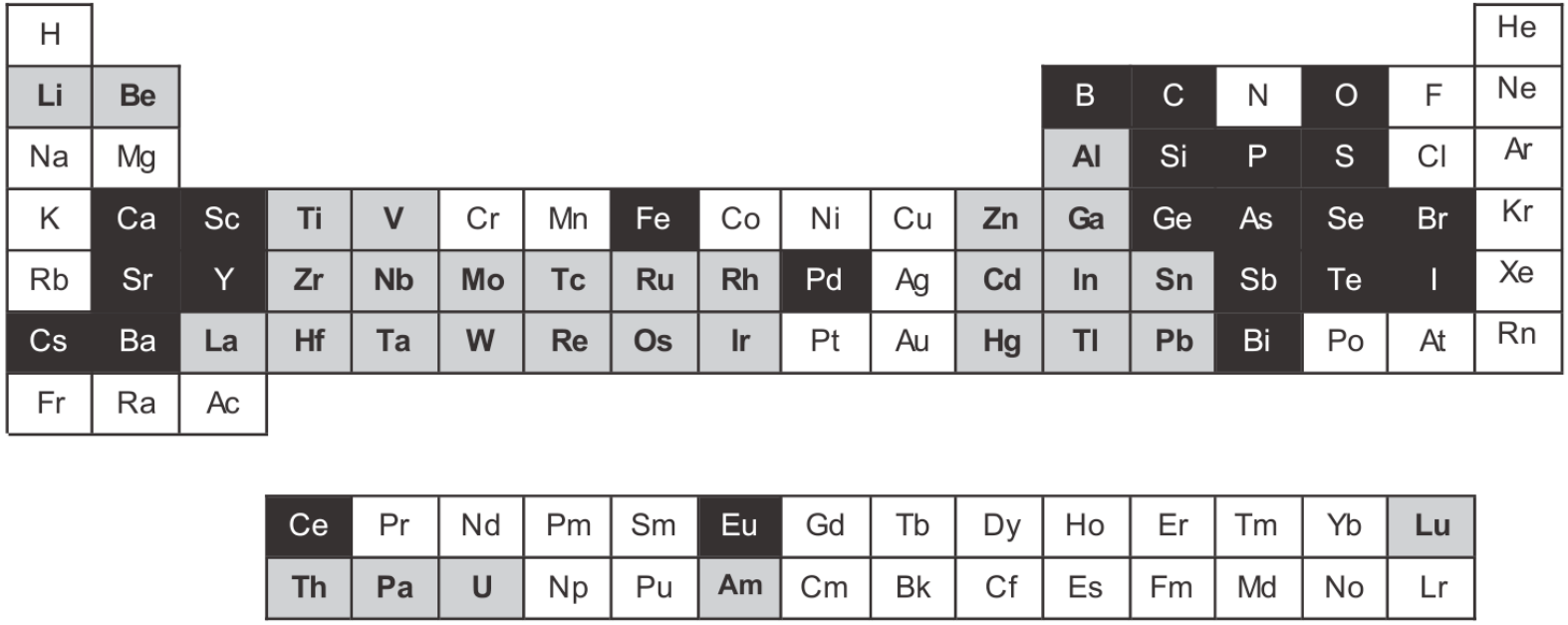

Figure 12.2 Periodic table of superconducting elements. Those in gray boxes will superconduct at ambient pressure in bulk form. Elements in black boxes have been shown to superconduct under pressure or as thin films.

Highest Temp element is Nb @9.25 K and ambient pressure.

Material	T_c (K)	Comment
Rh	0.0003	Lowest T_c of any superconducting element
Hg	4.153	First superconductor discovered in 1911
Pb	7.2	Highest-T_c type-I superconducting element
Nb	9.25	Highest-T_c type-II superconducting element
Li	0.004/20	Ambient/~30 GPa
Ca	21–25	Highest-T_c element ~220 GPa
Nb_3Sn	18	High-T_c intermetallic
Nb_3Ge	23.2	Highest-T_c intermetallic
NbO	1.5	First oxide superconductor, 1933
$SrTiO_{3-\delta}$	0.3	First perovskite superconductor
$BaPb_{1-x}Bi_xO_3$	13	First high-temperature superconductor of 1970s
$Ba_{0.6}K_{0.4}BiO_3$	34	Highest T_c of $BaBiO_3$-related systems
$La_{1.85}Ba_{0.15}CuO_4$	30	First cuprate superconductor, 1986
$La_{1.85}Sr_{0.15}CuO_4$ or $La_2CuO_{4.08}$	38	Highest-T_c "214" cuprate superconductor
$YBa_2Cu_3O_7$	93	First >77 K (N_2 boiling point) superconductor, 1987
$HgBa_2Ca_2Cu_3O_{8+x}$	134/164	Highest-T_c cuprate at ambient/elevated pressure
$Ba_{1-x}Sr_xCuO_2$	90	Infinite-layer cuprate
$Ca_{1-x}Sr_xCuO_2$	110	Highest-T_c ternary infinite-layer cuprate

Applied Magnetic Field

- Created by current through a coil:

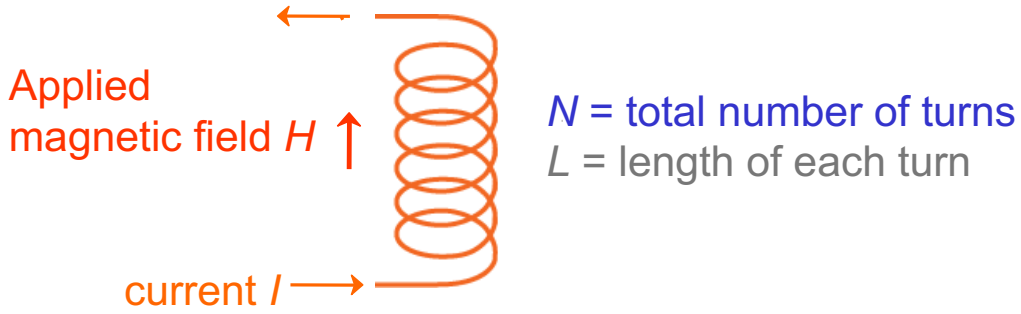

- Relation for the applied magnetic field, *H*:

$$H = \frac{N I}{L}$$

I: current

H: applied magnetic field
units = (ampere-turns/m)

- Here a Magnetic Field is the result of a current

Response to a Magnetic Field

- Magnetic induction results in the material

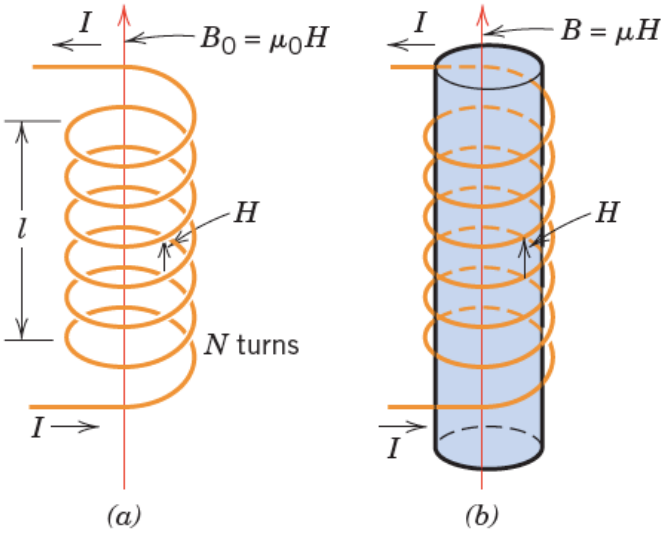

$$B_0 = \mu_0 H$$

$$B = \mu H$$

$$\mu_r = \frac{\mu}{\mu_0}$$

$$B = \mu_0 H + \mu_0 M$$

Contribution to the field due to magnetization of the solid

$$M = (\mu_r - 1)H$$

Quantity	Symbol	SI Units: Derived	SI Units: Primary
Magnetic induction (flux density)	B	tesla $(Wb/m^2)^a$	kg/s-C
Permeability of a vacuum	μ_0	henry/m^b	kg-m/C^2
Magnetic field strength	H	amp-turn/m	C/m-s
Magnetization	M (SI) I (cgs–emu)	amp-turn/m	C/m-s

Response to a Magnetic Field

- Magnetic susceptibility, χ (dimensionless)

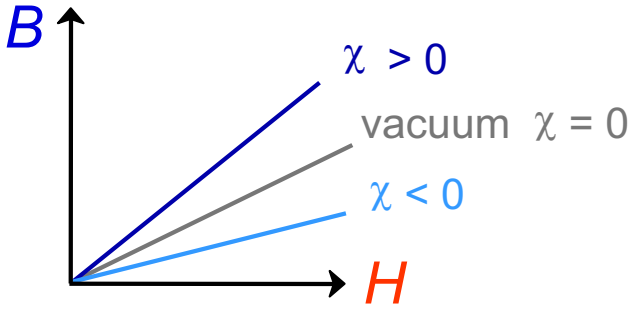

χ measures the material response relative to a vacuum.

$$B = \mu_0(H+M) = \mu_0(1+\chi_m)H = \mu H$$

$$M = \chi_m H$$

$$\chi_m = \mu_r - 1$$

Origins of Magnetic Moments

- Electrons produce magnetic moments:

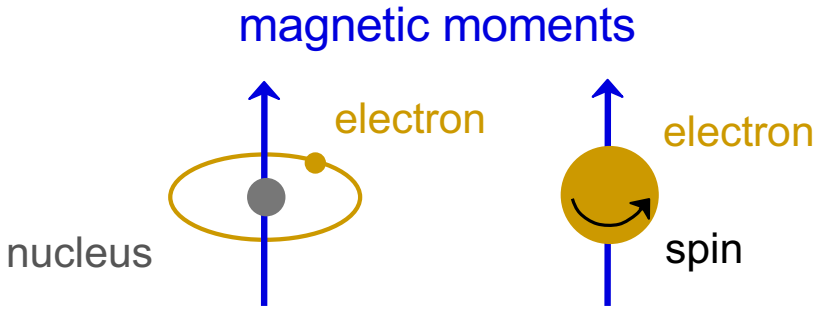

- Net magnetic moment:
  --sum of moments from all electrons.

- Three types of response...

Diamagnetism

- Present in all materials
- Electrons change their orbit to oppose applied field

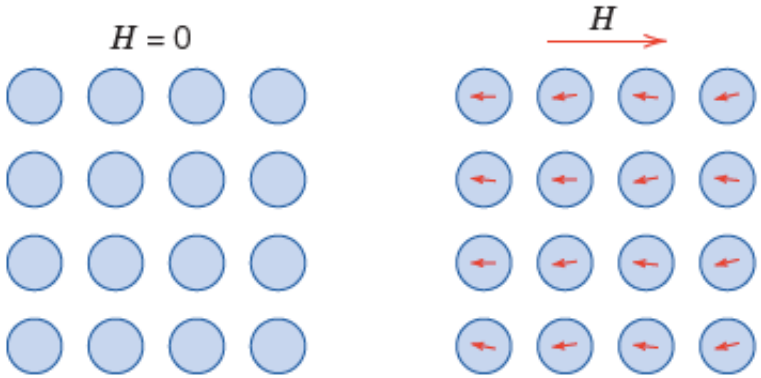

Paramagnetism

- Present in materials with unpaired electrons
- Electron spins align with applied field

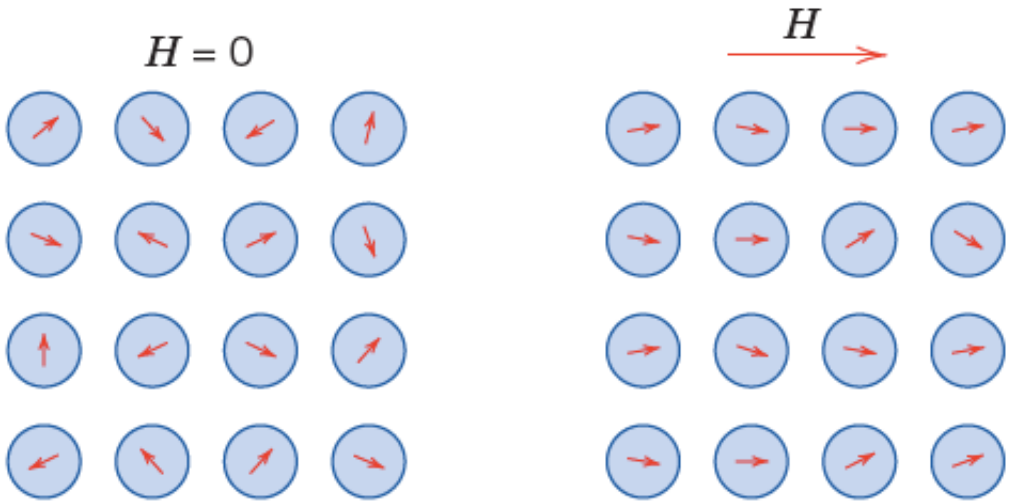

Ferromagnetism

- Spins couple and align with no applied field

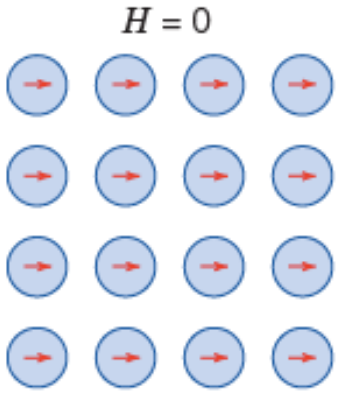

Table 14.1. Magnetic Constants of Some Materials at Room Temperature.

Material	χ (SI) unitless	χ (cgs) unitless	μ unitless	Type of magnetism
Low carbon steel	$\approx 5 \times 10^3$	3.98×10^2	5×10^3	
Fe–3%Si (grain-oriented)	4×10^4	3.18×10^3	4×10^4	Ferromagnetic
Ni–Fe–Mo (supermalloy)	10^6	7.96×10^4	10^6	

Antiferromagnetism

- Spins couple, align, and cancel

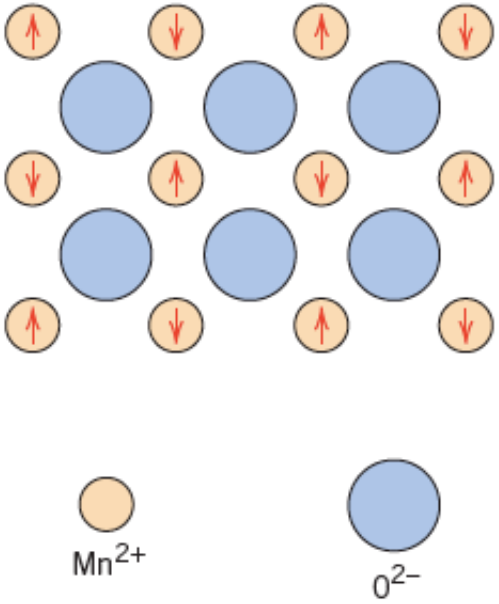

MnO

Table 14.1. Magnetic Constants of Some Materials at Room Temperature.

Material	χ (SI) unitless	χ (cgs) unitless	μ unitless	Type of magnetism
Bi	-165×10^{-6}	-13.13×10^{-6}	0.99983	
Ge	-71.1×10^{-6}	-5.66×10^{-6}	0.99992	
Au	-34.4×10^{-6}	-2.74×10^{-6}	0.99996	
Ag	-23.8×10^{-6}	-1.90×10^{-6}	0.99997	
Be	-23.2×10^{-6}	-1.85×10^{-6}	0.99998	Diamagnetic
Cu	-9.7×10^{-6}	-0.77×10^{-6}	0.99999	
Water	-9.14×10^{-6}	-0.73×10^{-6}	0.99999	
Si	-4.1×10^{-6}	-0.32×10^{-6}	0.99999	
Superconductors[a]	-1.0	$\sim -8 \times 10^{-2}$	0	
β-Sn	$+2.4 \times 10^{-6}$	$+0.19 \times 10^{-6}$	1	
Al	$+20.7 \times 10^{-6}$	$+1.65 \times 10^{-6}$	1.00002	
W	$+77.7 \times 10^{-6}$	$+6.18 \times 10^{-6}$	1.00008	Paramagnetic
Pt	$+264.4 \times 10^{-6}$	$+21.04 \times 10^{-6}$	1.00026	
Low carbon steel	$\approx 5 \times 10^{3}$	3.98×10^{2}	5×10^{3}	
Fe–3%Si (grain-oriented)	4×10^{4}	3.18×10^{3}	4×10^{4}	Ferromagnetic
Ni–Fe–Mo (supermalloy)	10^{6}	7.96×10^{4}	10^{6}	

Are Superconductors Special?

(1) Resistivity of Ag is 10^{-11} ohm m at I **K** , for superconductors is 10^{-25}

Are Superconductors Special?

(2) Different Magnetic Properties: Ag is a very weak diagmagnet, superconductors are perfect diamagnet up to a critical field H_c

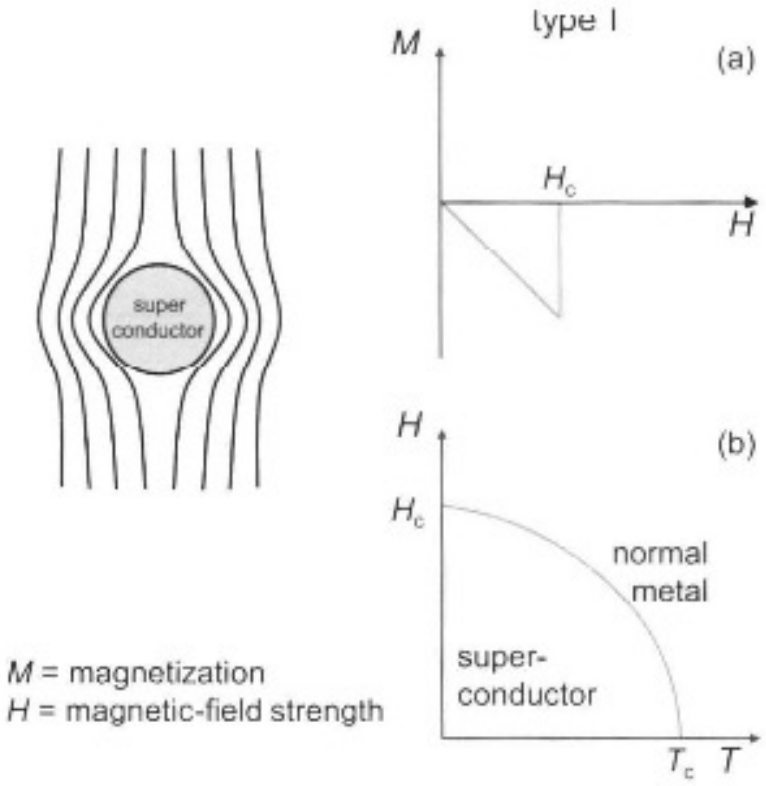

(3) Thermodynamic Analysis reviews Tc is associated with a 2nd order transition

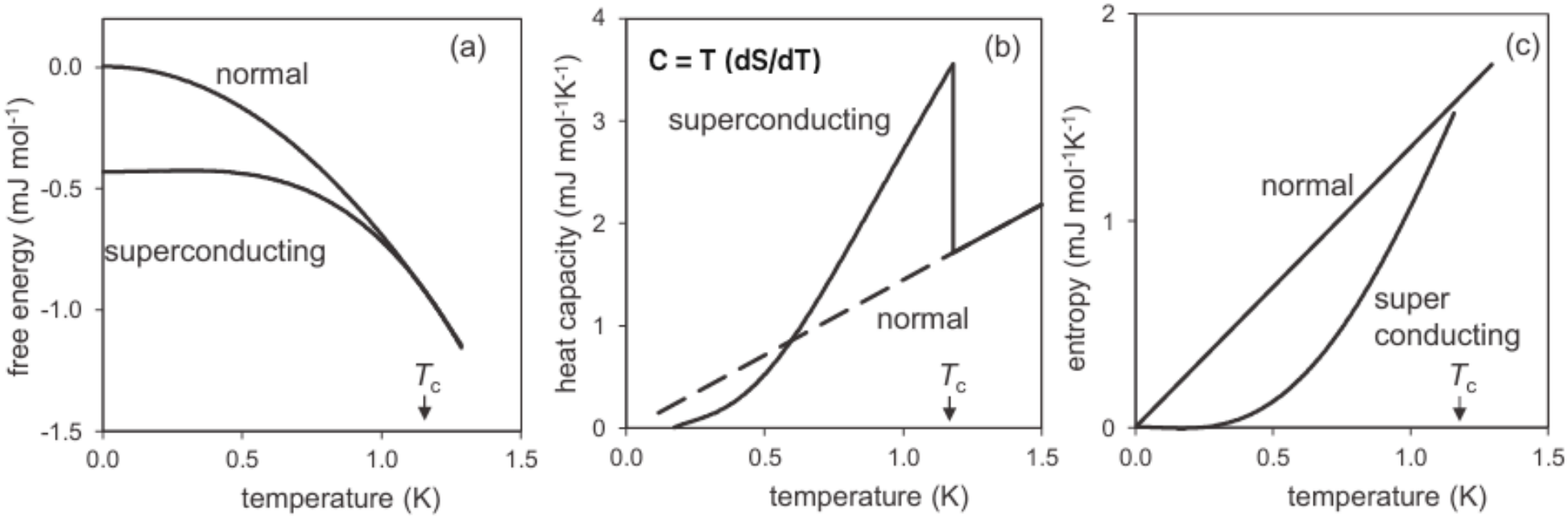

Figure 12.5 (a) Free energy, (b) heat capacity, and (c) entropy of Al in the superconducting and normal states of aluminum. Parts (a) and (c) after [5].

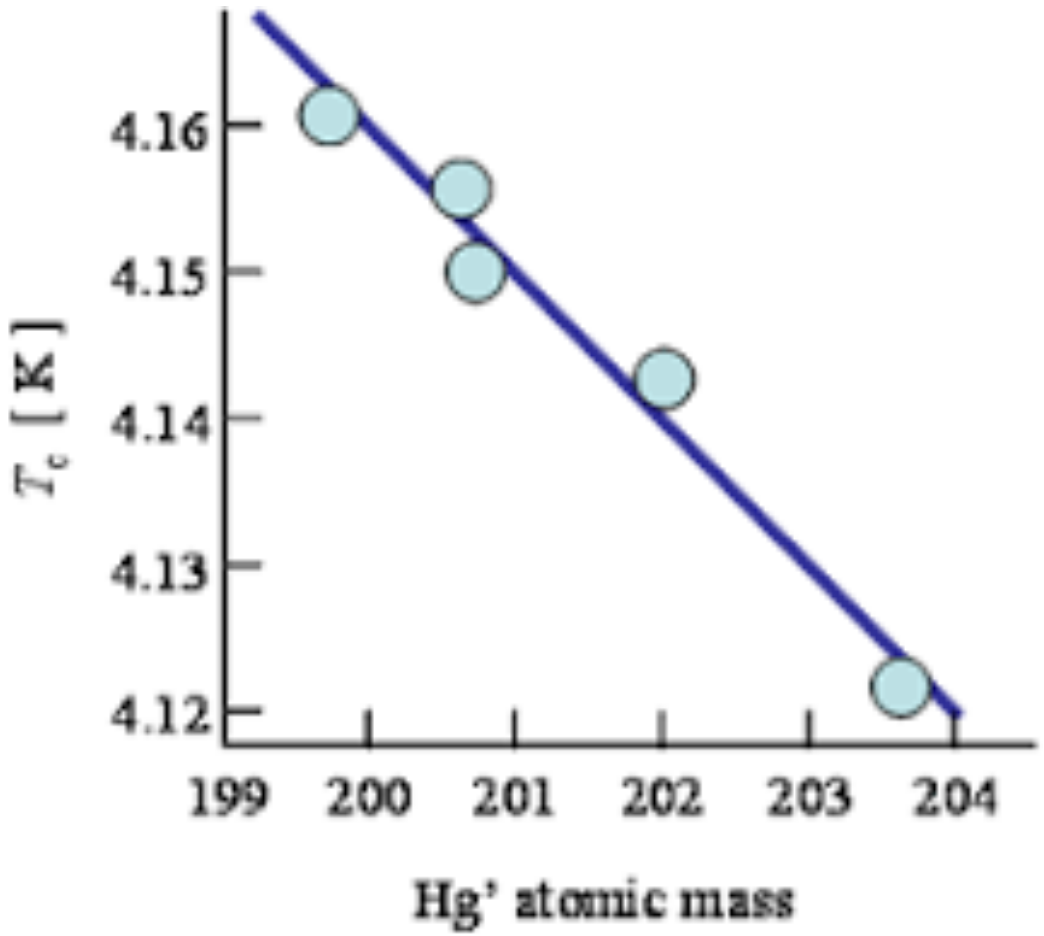

Fig. 13 Hg's isotopic effect

PHYSICAL REVIEW VOLUME 108, NUMBER 5 DECEMBER 1, 1957

Theory of Superconductivity*

J. BARDEEN, L. N. COOPER,† AND J. R. SCHRIEFFER‡
Department of Physics, University of Illinois, Urbana, Illinois
(Received July 8, 1957)

A theory of superconductivity is presented, based on the fact that the interaction between electrons resulting from virtual exchange of phonons is attractive when the energy difference between the electrons states involved is less than the phonon energy, $\hbar\omega$. It is favorable to form a superconducting phase when this attractive interaction dominates the repulsive screened Coulomb interaction. The normal phase is described by the Bloch individual-particle model. The ground state of a superconductor, formed from a linear combination of normal state configurations in which electrons are virtually excited in pairs of opposite spin and momentum, is lower in energy than the normal state by amount proportional to an average $(\hbar\omega)^2$, consistent with the isotope effect. A mutually orthogonal set of excited states in one-to-one correspondence with those of the normal phase is obtained by specifying occupation of certain Bloch states and by using the rest to form a linear combination of virtual pair configurations. The theory yields a second-order phase transition and a Meissner effect in the form suggested by Pippard. Calculated values of specific heats and penetration depths and their temperature variation are in good agreement with experiment. There is an energy gap for individual-particle excitations which decreases from about $3.5kT_c$ at $T=0°K$ to zero at T_c. Tables of matrix elements of single-particle operators between the excited-state superconducting wave functions, useful for perturbation expansions and calculations of transition probabilities, are given.

The Nobel Prize in Physics 1972

"for their jointly developed theory of superconductivity, usually called the BCS-theory"

John Bardeen

Leon Neil Cooper

John Robert Schrieffer

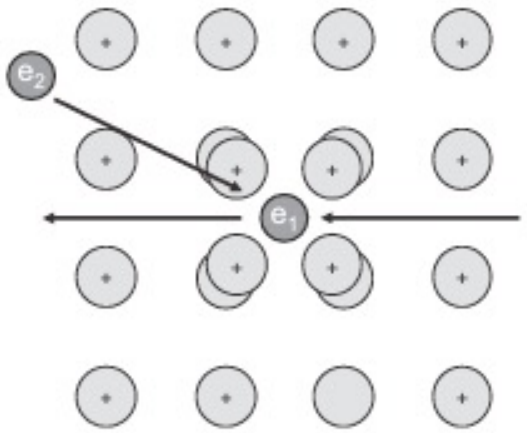

Figure 12.6 (a) Real-space illustration of how electron–phonon coupling in a simple metal system can lead to attractive interaction between two electrons.[9] (b) Virtual-phonon exchange behind Cooper-pair formation.

Electron Pairing Distance Estimate

Since electrons move much faster than the heavier metal ions, there is a time delay between the motion of the first electron (which distorts the lattice) and the subsequent attraction of the second electron. To estimate the distance **d** the first electron has traveled by the time the second is attracted, we use:

- $\mathbf{v_n}$: velocity of an electron at the Fermi level
- **ω_D**: Debye angular frequency, which sets how fast the lattice can respond

The estimated distance is

$$\mathbf{d = v_F (2\pi / \omega_D)}$$

For aluminum:

- $v_F \approx 2\times10^{6}$ m/s
- $\omega_D \approx 5\times10^{13}$ s^{-1}

This gives:

d ≈ 2500 Å

This distance is large compared with atomic spacing, so Coulomb repulsion between the electrons is negligible, especially due to screening by the positively charged metal ions.

Conservation of momentum leads to the relationships:

$$k_1 = k_1' + q \text{ and } k_2 + q = k_2'$$

$$(k_1 + k_2) = (k_1' + q) + (k_2' - q)$$

$$k_1 + k_2 = k_1' + k_2' = k_0$$

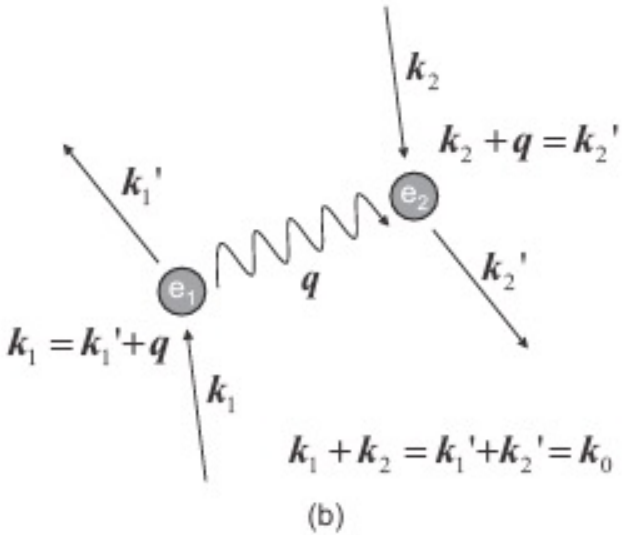

Figure 12.6 (a) Real-space illustration of how electron–phonon coupling in a simple metal system can lead to attractive interaction between two electrons.[9] (b) Virtual-phonon exchange behind Cooper-pair formation.

Electron Pairing in k-Space

To form a Cooper pair through phonon exchange, each electron must scatter into a different quantum state. The Pauli exclusion principle limits which states are available: electrons deep below the Fermi energy EF cannot scatter because all nearby states are already occupied. Only electrons close enough to EF have empty states available.

A phonon of energy ħω can only change an electron's energy by at most ħω. Therefore, an electron can scatter only if there is an *unoccupied* state within that energy range. When you combine this with Pauli exclusion, the result is that only electrons within an energy window of order ħω around EF can participate in pairing.

In k-space, this allowed energy window corresponds to a thin shell of states surrounding the Fermi surface, with thickness δk determined by ħω. Only electrons whose wave vectors fall within this narrow shell can experience the phonon-mediated attraction, as shown schematically in Figure 12.7.

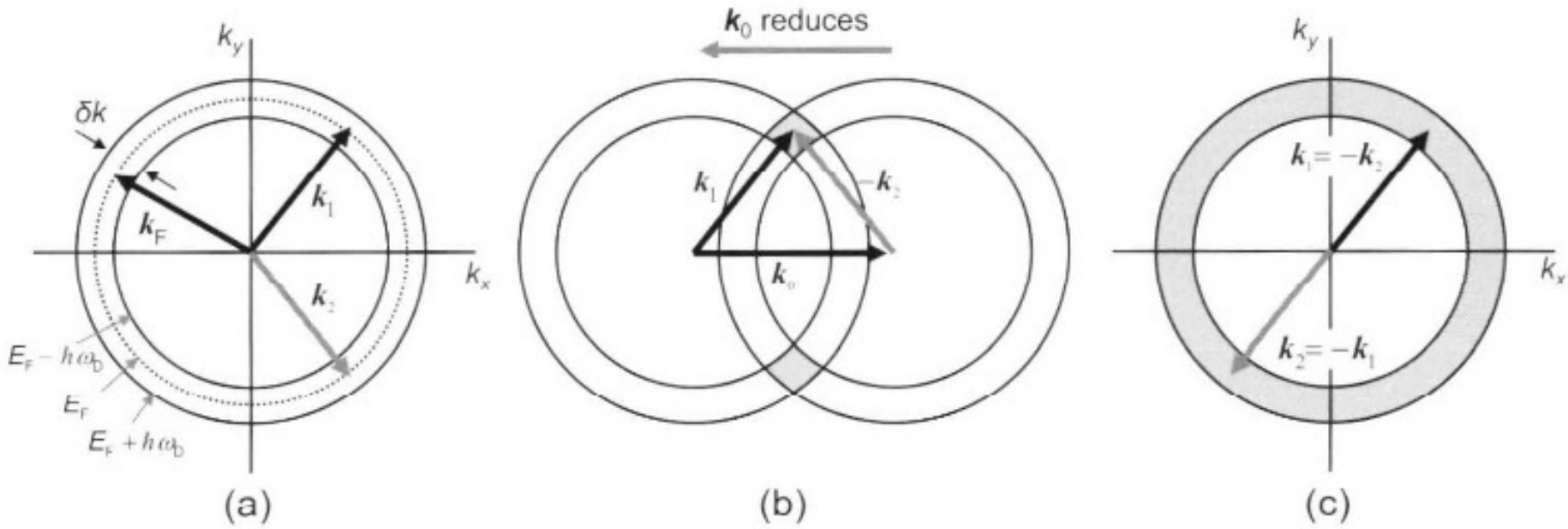

Figure 12.7 (a) A k-space sketch of a spherical shell of states within δk of Fermi level k_F. Electrons with arbitrary wave vectors $\boldsymbol{k}_1$ and $\boldsymbol{k}_2$ are shown. The change in $\boldsymbol{k}_1$ on phonon exchange is restricted to a small area determined by δk. (b) The overall condition of $\boldsymbol{k}_1 + \boldsymbol{k}_2 = \boldsymbol{k}_0$ for virtual phonon exchange can be represented geometrically by two such shells offset by $\boldsymbol{k}_0$. For a given value of $\boldsymbol{k}_0$ the overlap region (shaded) gives the states that can be involved in coupling. The maximum coupling will occur when the two shells overlap such that $\boldsymbol{k}_0 = 0$ and $\boldsymbol{k}_1 = -\boldsymbol{k}_2$.

Why $k_o = 0$ gives the most possible pairs

If $k_o = 0$, then the rule becomes:

$k_2 = -k_1$

That means **every state k in the shell automatically has a partner −k** that is also in the shell.

This doubles your options: every point on the Fermi surface has a matching point directly opposite it. So the number of available pair states is maximized.

If k_o is not zero (say, k_o is some nonzero vector), then the partner of k_1 is $k_2 = k_o - k_1$. Many of those points **don't lie in the allowed shell anymore**, so the number of available pairs drops.

$k_0 = k_1 + k_2$, so $k_0 = 0$ means:

$k_1 + k_2 = 0 \rightarrow k_2 = -k_1$

In other words, the two electrons in a Cooper pair must have **equal and opposite momenta**.

Because electrons are fermions, their spins must also be opposite for the overall two-electron wavefunction to be allowed. So a Cooper pair consists of states:

(k, ↑) and (−k, ↓)

This is called **s-wave pairing**, which is the type found in conventional (BCS) superconductors.

Finally, a Cooper pair is not like two electrons locked together in a fixed chemical bond. Instead, it is a dynamic quantum state in which many electrons near the Fermi surface continuously exchange phonons and momentarily form paired states with opposite momenta and opposite spins.

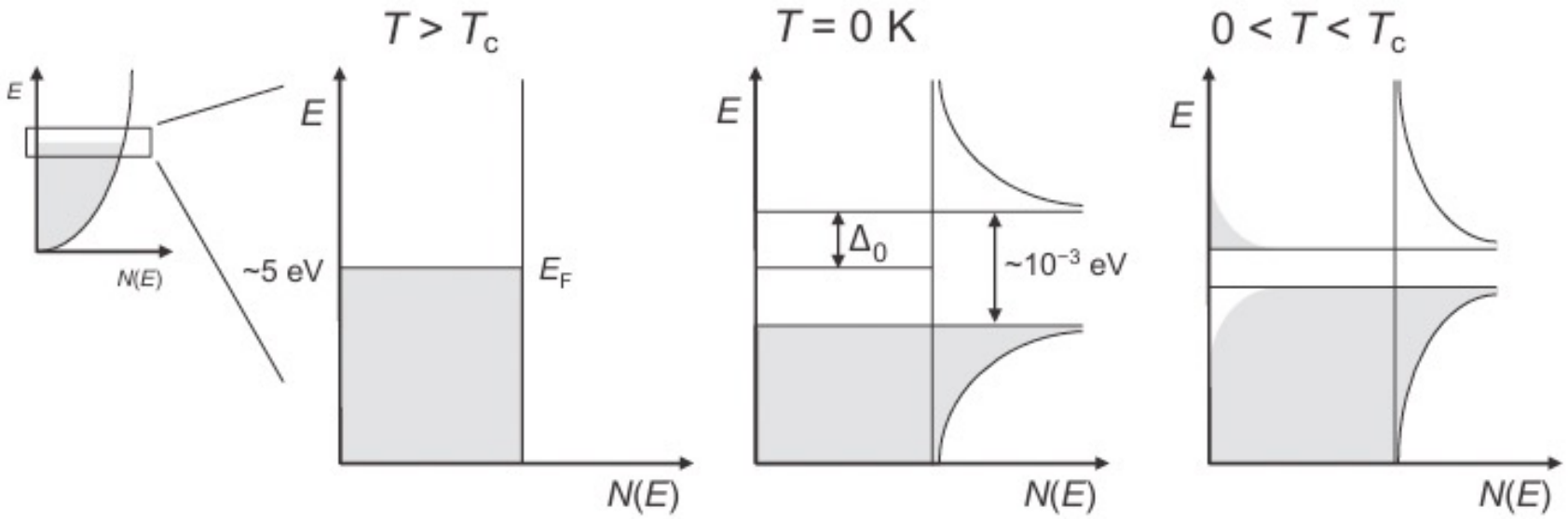

Figure 12.8 DOS plot of a metal close to E_F in its normal and superconducting states. In the superconducting state, peaks appear in $N(E_F)$ just below and above the gap. Away from E_F, the DOS of the superconductor is similar to a normal metal. At $T > 0$ K, there is some occupancy of normal states above the gap.

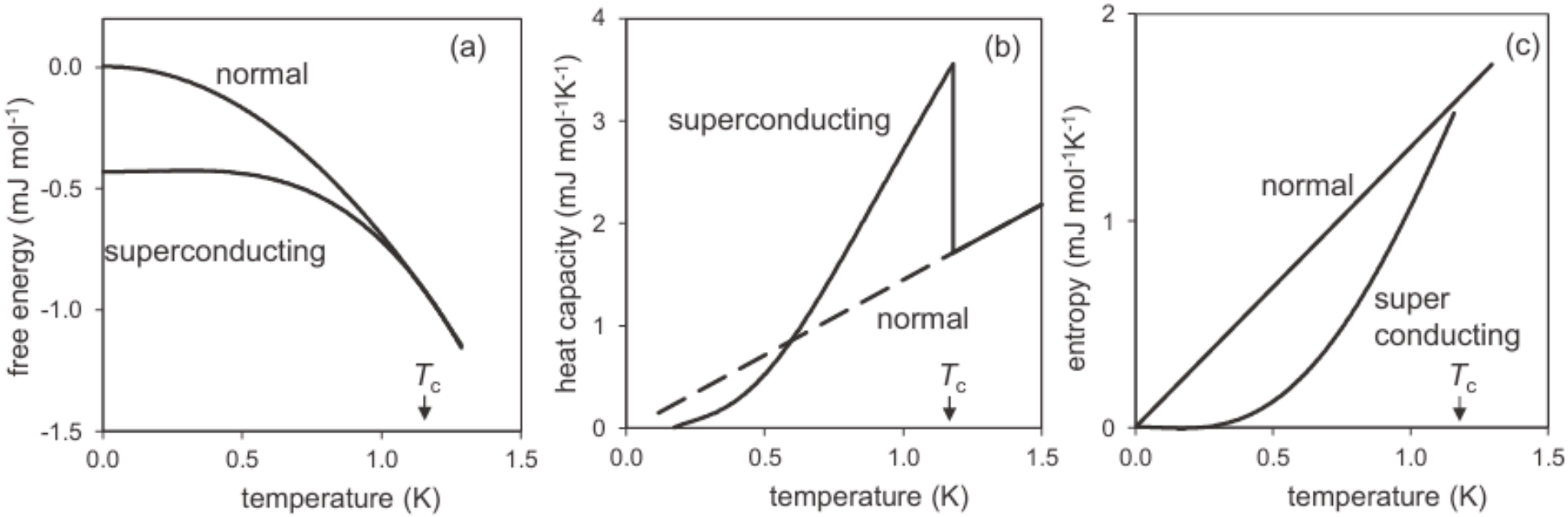

Figure 12.5 (a) Free energy, (b) heat capacity, and (c) entropy of Al in the superconducting and normal states of aluminum. Parts (a) and (c) after [5].

BCS Prediction for the Zero-Temperature Gap and Tc

$$\Delta_0 = \frac{\hbar\omega_D}{\sinh\left[\frac{1}{N(E_F)\,V}\right]} \approx 2\hbar\omega_D\, e^{-1/(N(E_F)V)}$$

- $N(E_F)$ is the density of states at the Fermi level
- V is the electron–phonon coupling strength
- ω_D is the Debye frequency

Typical experimental measurements the zero temp energy gap are $\Delta_0 \approx 5\times10^{-4}\ \text{eV}$

BCS Theory further predicts that $2\Delta_0 = 3.52kT_c$

$$T_c = \frac{2\Delta_0}{3.52\,k_B} = \frac{2(5\times10^{-4}\,\text{eV})}{3.52\,(8.617\times10^{-5}\,\text{eV/K})} \approx 3.3\ \text{K}$$

BCS prediction evaluated at Tc yields:

$$T_\mathrm{c} = 1.14 \frac{\hbar\omega_\mathrm{D}}{k} \mathrm{e}^{-1/N(E_\mathrm{F})\cdot V'}$$

- The BCS expression for T_c shows that it scales with the Debye frequency ω_D.

  This explains the **isotope effect** and why materials containing light elements (such as MgB_2) can have high T_c due to their high phonon frequencies.

- A larger electron–phonon interaction V leads to a higher T_c.

  This explains why **good normal conductors** (Cu, Ag, Au), which have weak electron-phonon coupling, are poor superconductors, while **poor normal conductors** (often oxides with stronger coupling) can be good superconductors.

Why Superconductors Have Zero Resistance

- In a superconductor, **all Cooper pairs occupy the same quantum state**, behaving as a single coherent ensemble rather than individual electrons.

Temperature Milestones for Superconductors

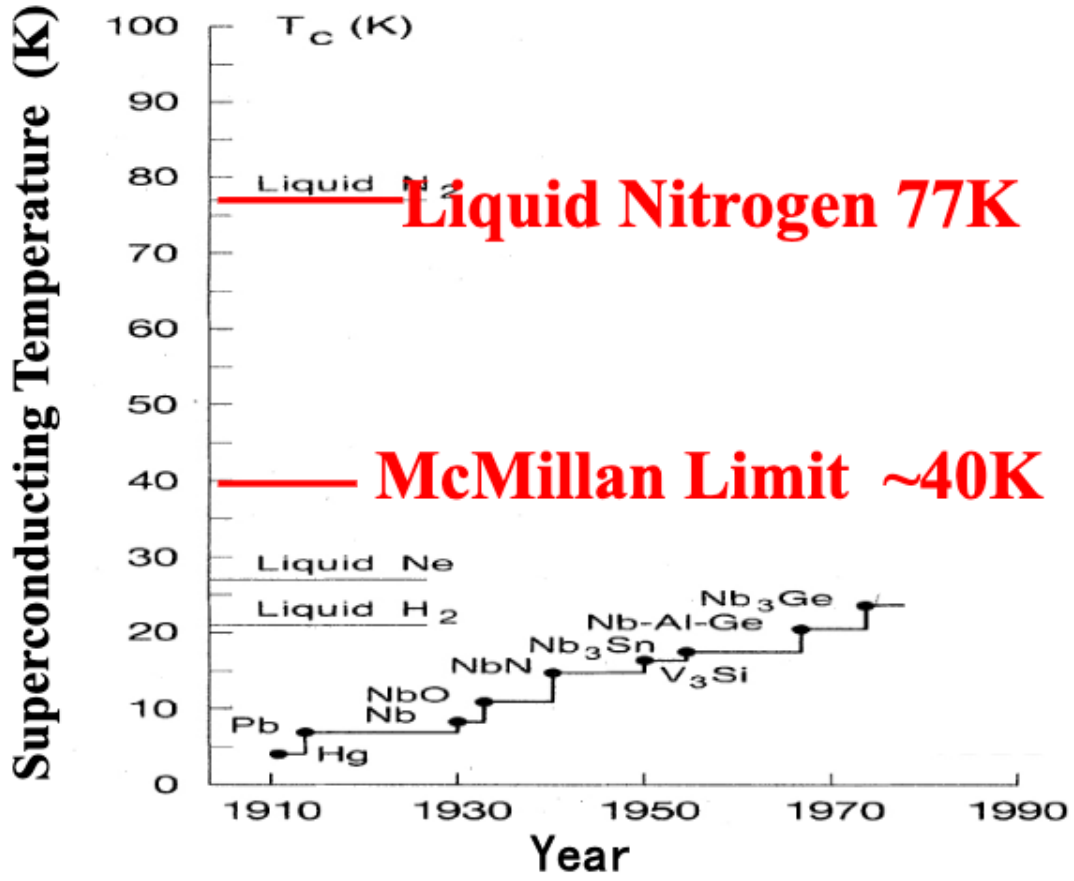

Discovery of Superconductivity in Copper-Oxide Compounds

Z. Phys. B – Condensed Matter 64, 189–193 (1986)

Condensed Matter
Zeitschrift für Physik B

Possible High T_c Superconductivity in the Ba – La – Cu – O System

J.G. Bednorz and K.A. Müller
IBM Zürich Research Laboratory, Rüschlikon, Switzerland

Received April 17, 1986

The Nobel Prize in Physics 1987

"for their important break-through in the discovery of superconductivity in ceramic materials"

J. Georg Bednorz

K. Alexander Müller

Metallic, oxygen-deficient compounds in the Ba – La – Cu – O system, with the composition $Ba_xLa_{5-x}Cu_5O_{5(3-y)}$ have been prepared in polycrystalline form. Samples with $x=1$ and 0.75, $y>0$, annealed below 900 °C under reducing conditions, consist of three phases, one of them a perovskite-like mixed-valent copper compound. Upon cooling, the samples show a linear decrease in resistivity, then an approximately logarithmic increase, interpreted as a beginning of localization. Finally an abrupt decrease by up to three orders of magnitude occurs, reminiscent of the onset of percolative superconductivity. The highest onset temperature is observed in the 30 K range. It is markedly reduced by high current densities. Thus, it results partially from the percolative nature, bute possibly also from $2D$ superconducting fluctuations of double perovskite layers of one of the phases present.

Superconductivity at 93 K in a New Mixed-Phase Y-Ba-Cu-O Compound System at Ambient Pressure

M. K. Wu, J. R. Ashburn, and C. J. Torng
Department of Physics, University of Alabama, Huntsville, Alabama 35899

and

P. H. Hor, R. L. Meng, L. Gao, Z. J. Huang, Y. Q. Wang, and C. W. Chu[(a)]
Department of Physics and Space Vacuum Epitaxy Center, University of Houston, Houston, Texas 77004
(Received 6 February 1987; Revised manuscript received 18 February 1987)

A stable and reproducible superconductivity transition between 80 and 93 K has been unambiguously observed both resistively and magnetically in a new Y-Ba-Cu-O compound system at ambient pressure. An estimated upper critical field $H_{c2}(0)$ between 80 and 180 T was obtained.

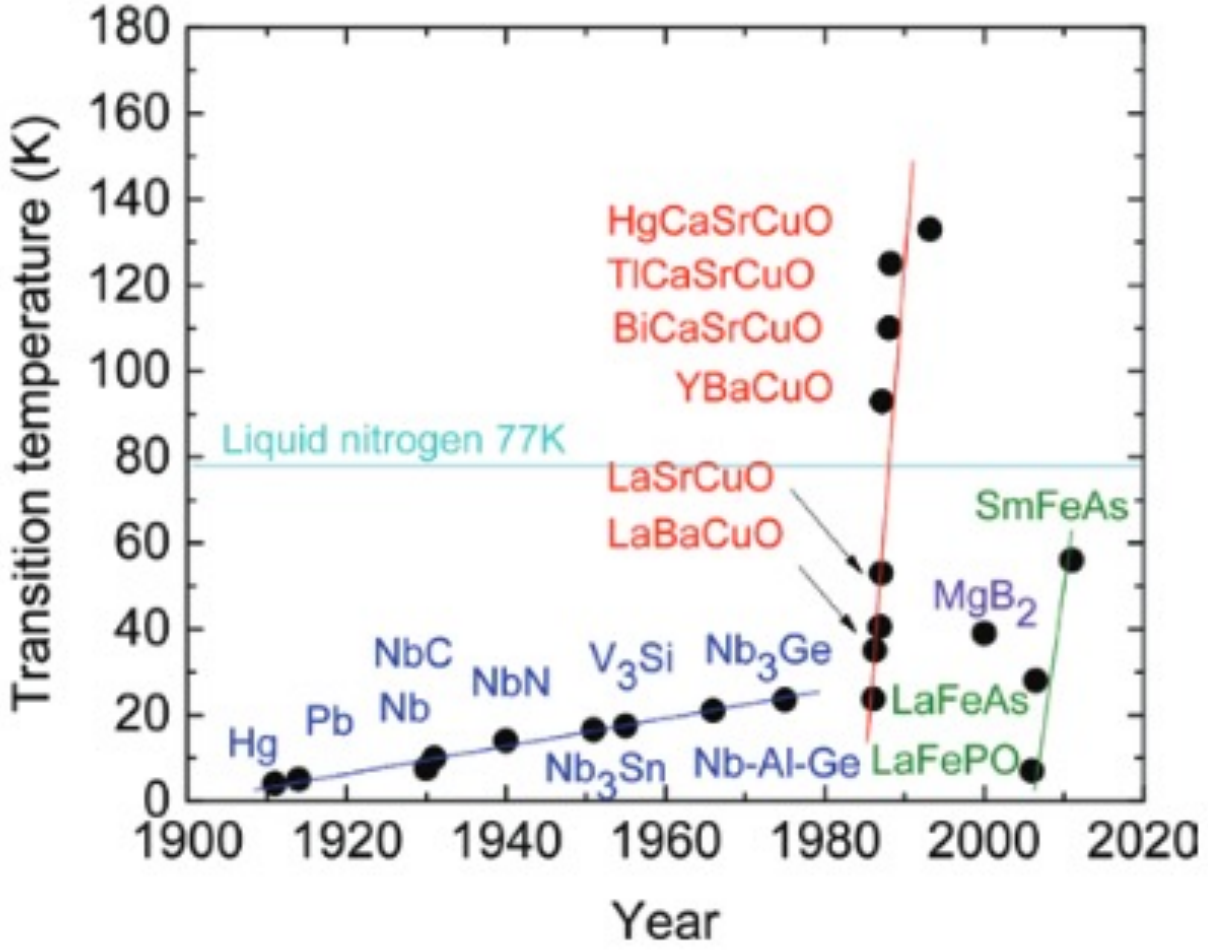
Transition temperature (K)
Year
Liquid nitrogen 77K
HgCaSrCuO
TlCaSrCuO
BiCaSrCuO
YBaCuO
LaSrCuO
LaBaCuO
SmFeAs
MgB2
LaFeAs
LaFePO
Hg
Pb
Nb
NbC
NbN
V3Si
Nb3Ge
Nb3Sn
Nb-Al-Ge

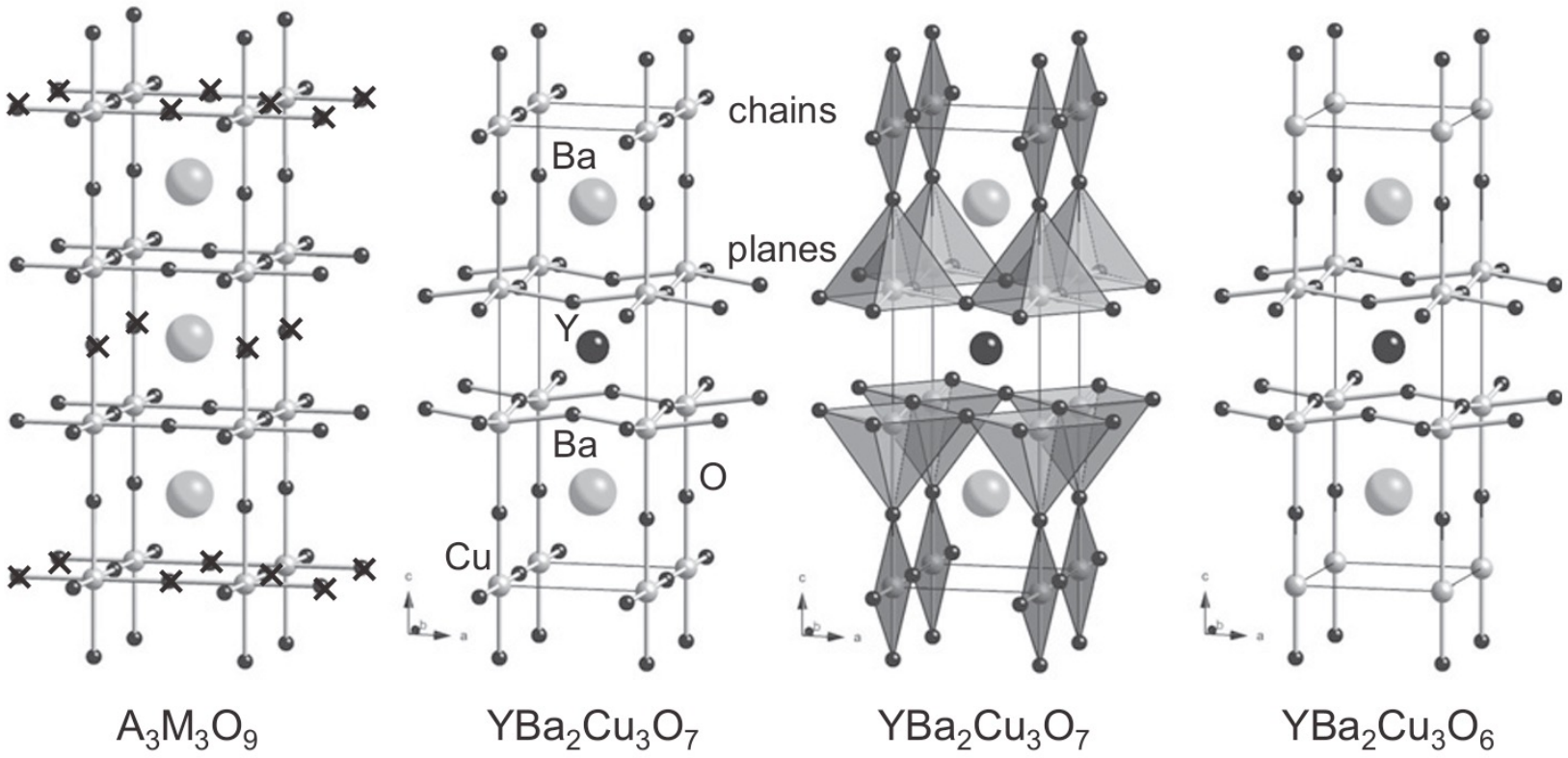

Figure 12.16 A hypothetical triple perovskite structure $A_3M_3O_9$. Deleting two oxygens per unit cell (crosses) leads to $YBa_2Cu_3O_7$, shown in ball-and-stick and polyhedral views. Deleting a further oxygen leads to $YBa_2Cu_3O_6$.

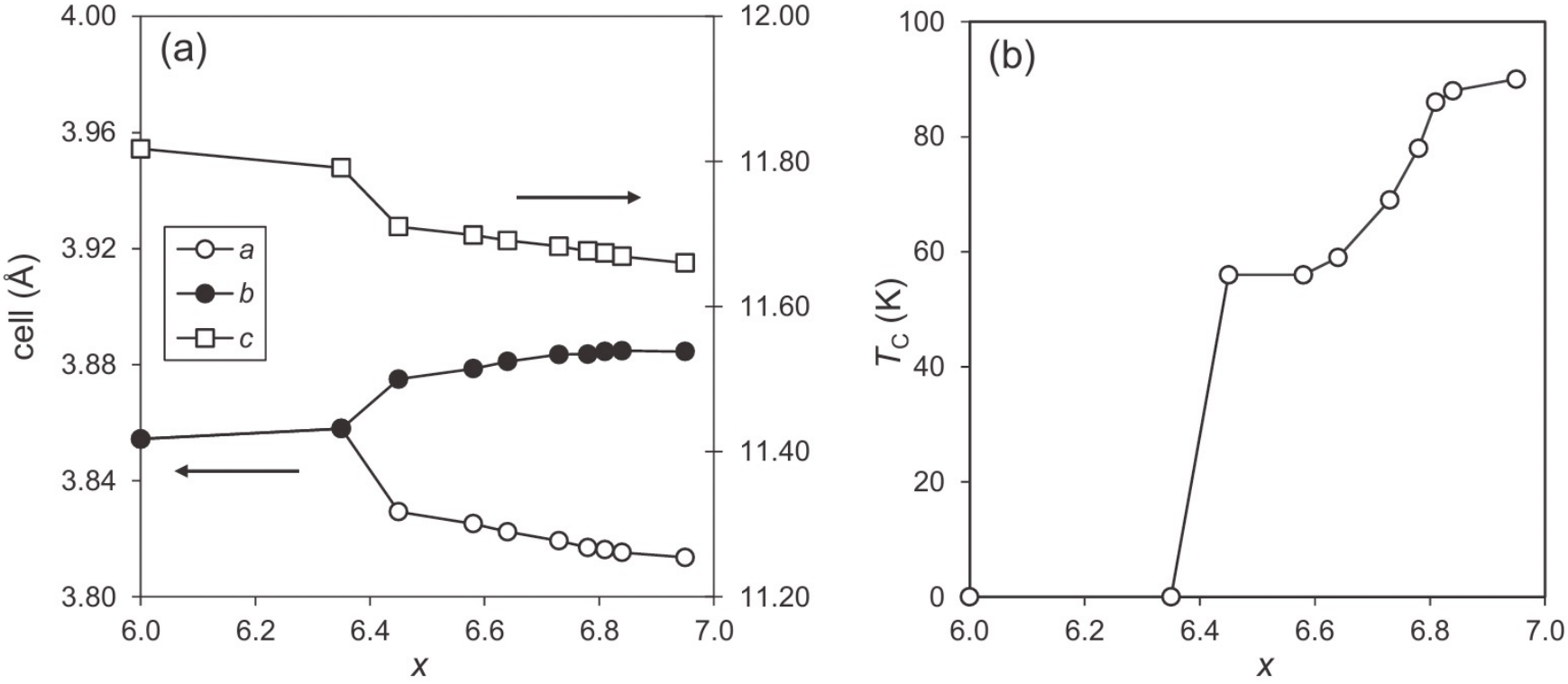

Figure 12.17 The dependence of (a) unit-cell parameters and (b) T_c on oxygen content for a series of $YBa_2Cu_3O_x$ samples. Data from [27].

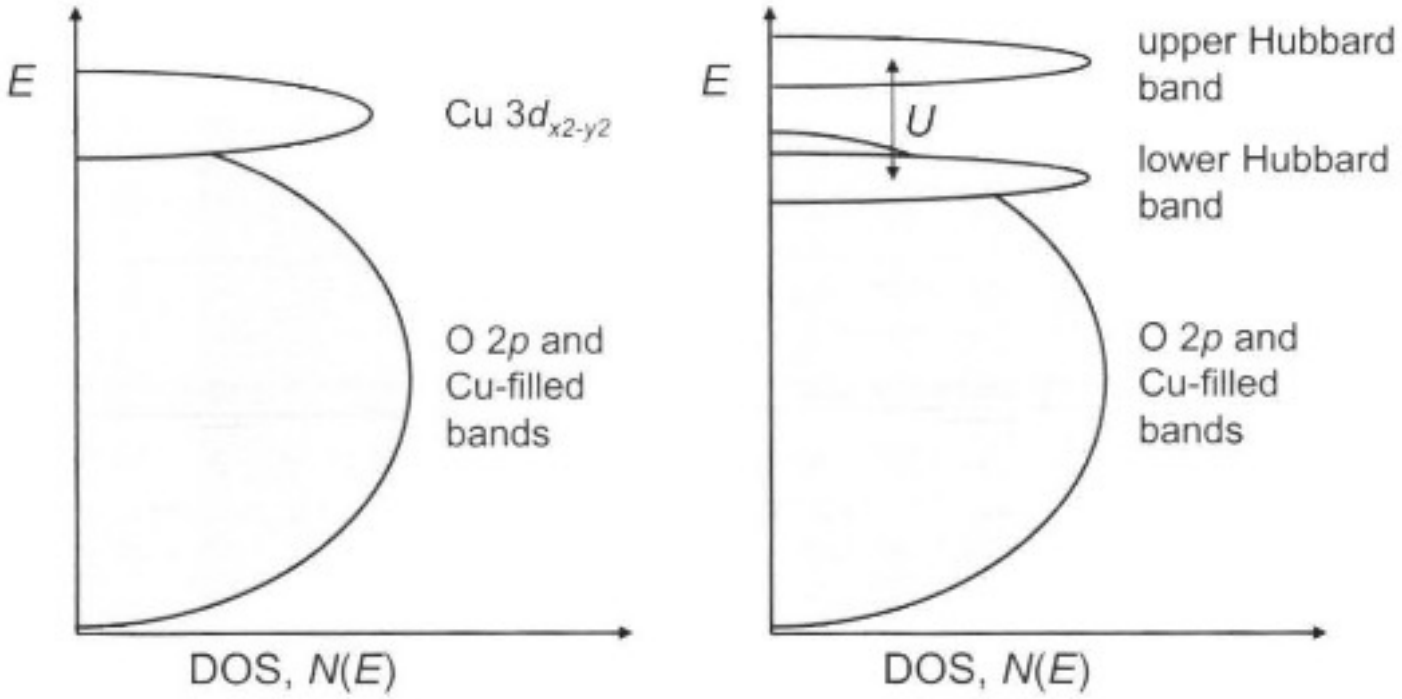

Figure 12.21 Left: Schematic density-of-states plots for $CuO_{4/2}$ planes; Right: Splitting of the $d_{x^2-y^2}$ into an upper and lower Hubbard band due to energy cost of electron pairing.

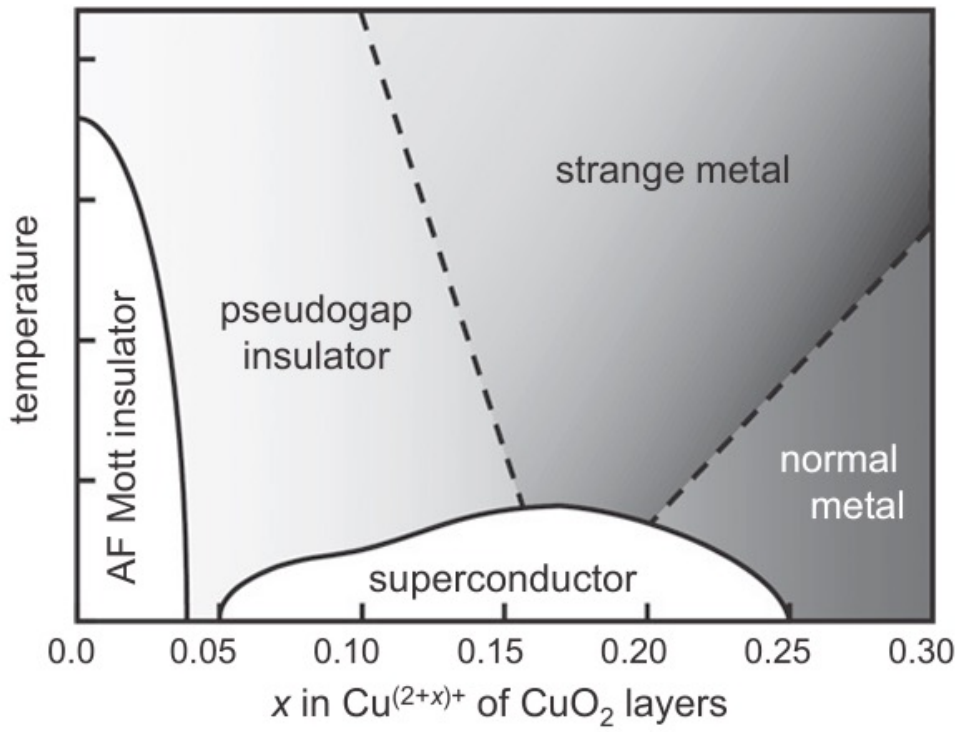

Figure 12.22 A generic phase diagram for hole-doped cuprate superconductors. Dashed lines separate regions where there are poorly defined changes in electronic behavior.

Pairing seems to come from electronic interactions, not phonons

In ordinary superconductors, electrons attract each other indirectly by distorting the lattice (phonons). In cuprates, that is not strong enough to explain T_c near 100 K.

Instead, the starting point is that the undoped cuprate is an antiferromagnetic Mott insulator: neighboring Cu spins strongly prefer to be opposite. When you dope holes into this system, you
• destroy long-range antiferromagnetic order
• but keep strong, short-range "up–down" tendencies that fluctuate in space and time

These time-dependent local antiferromagnetic patterns are what people mean by spin fluctuations.

They act as a kind of magnetic glue:
• an electron moving through the lattice disturbs the spin background
• another electron can lower its energy by moving in a way that fits this disturbed pattern
• the net effect is an effective attraction between electrons, even though the bare interaction is repulsive

So instead of an "electron–phonon" attraction, cuprates likely have an "electron–spin-fluctuation" attraction that binds electrons into Cooper pairs.

CuO_2^{2-} Sheet

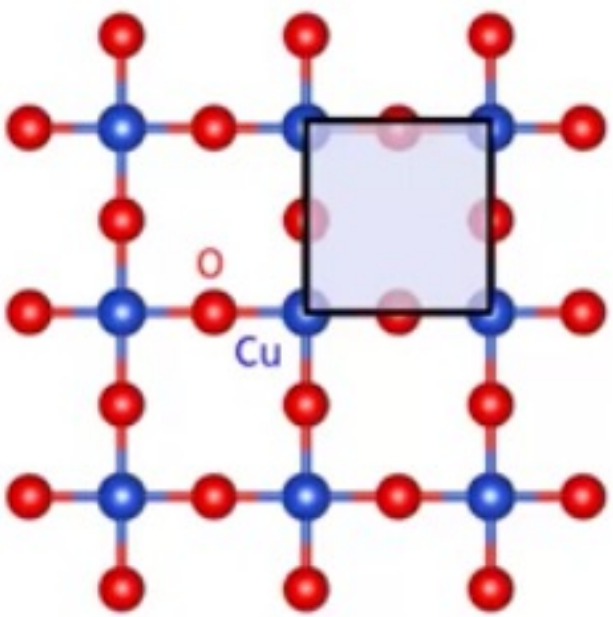

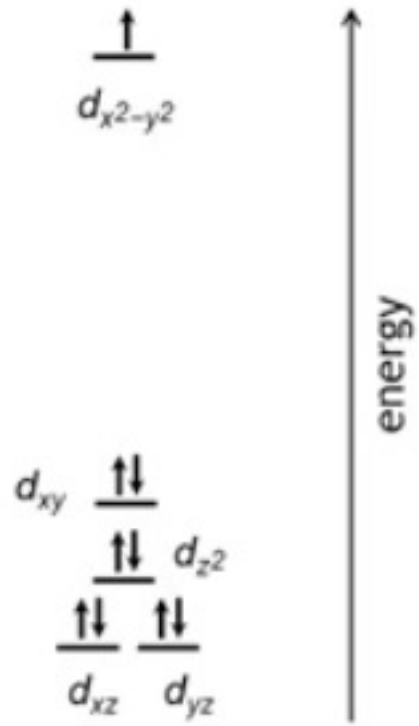

d-orbital energies
square planar Cu^{2+}

MO Diagram → DOS Plot

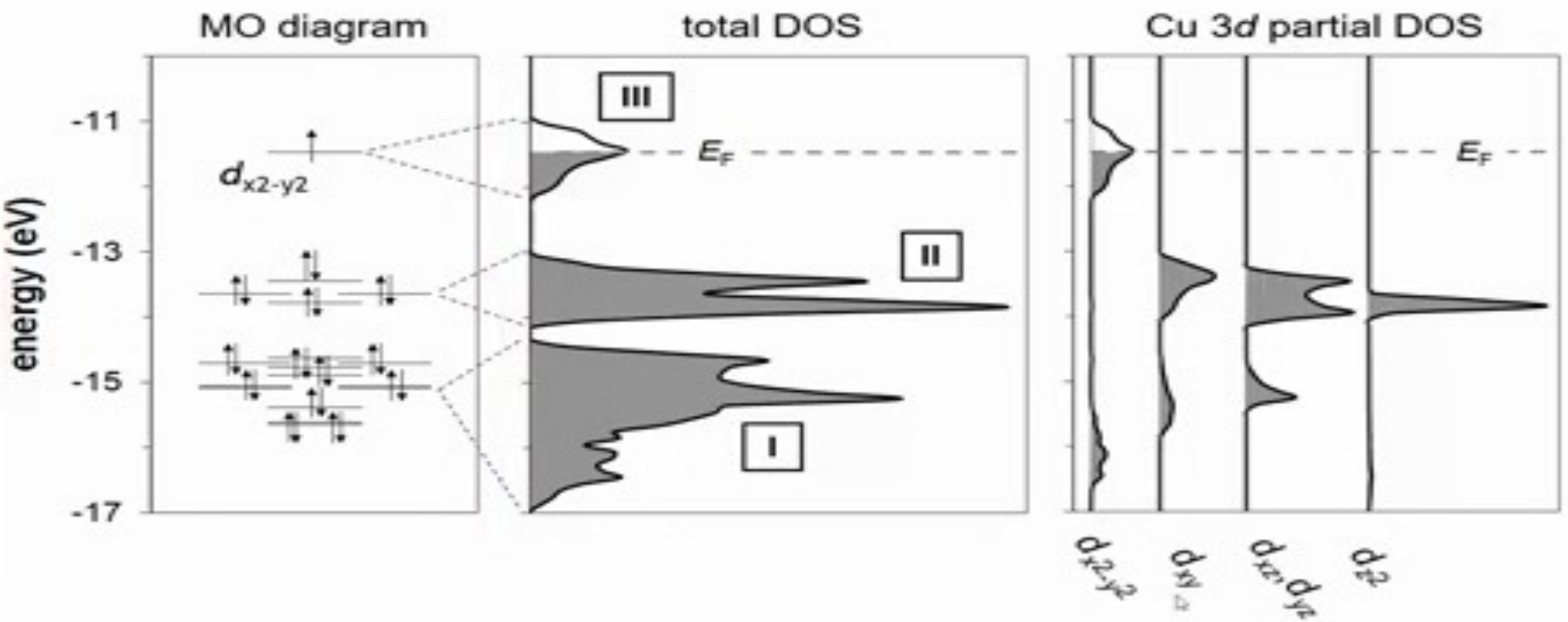

I — O 2p nonbonding and Cu-O bonding

II — Cu 3d-O 2p π antibonding

III — Cu 3d-O 2p σ antibonding

1987 P.W. Anderson RVB

The Resonating Valence Bond State in La2CuO4 and Superconductivity : Science 235, 1196

"The appropriate model seems to be the basic nearly half-filled Hubbard model"

$$H = -t \sum_{<i,j>\sigma} (c^{\dagger}_{i\sigma} c_{j\sigma} + c^{\dagger}_{j\sigma} c_{i\sigma}) + U \sum_{i} n_{i\uparrow} n_{i\downarrow}$$

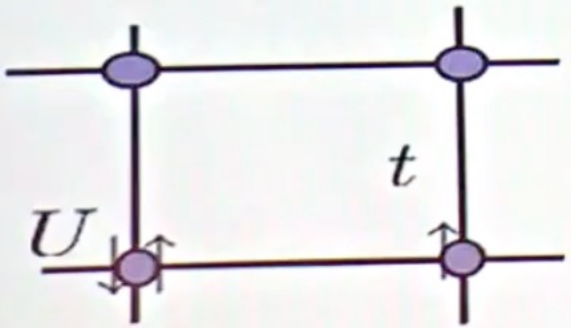

Coexistence of superconductivity with partially filled stripes in the Hubbard model

Hao Xu†, Chia-Min Chung†, Mingpu Qin, Ulrich Schollwöck, Steven R. White, Shiwei Zhang*

READ THE FULL ARTICLE AT
https://doi.org/10.1126/science.adh7691

Illustration of the ground-state properties of the *t*-*t*′-*U* Hubbard model. Dome-like structures in the superconducting order parameter resemble the T_c domes in the cuprates. With electron doping, superconductivity is accompanied by antiferromagnetic Néel correlations. With hole doping, superconductivity coexists with antiferromagnetic correlations that are modulated by a wavelength smaller than 2/doping, with moderate hole-density correlation peaks at the nodes.

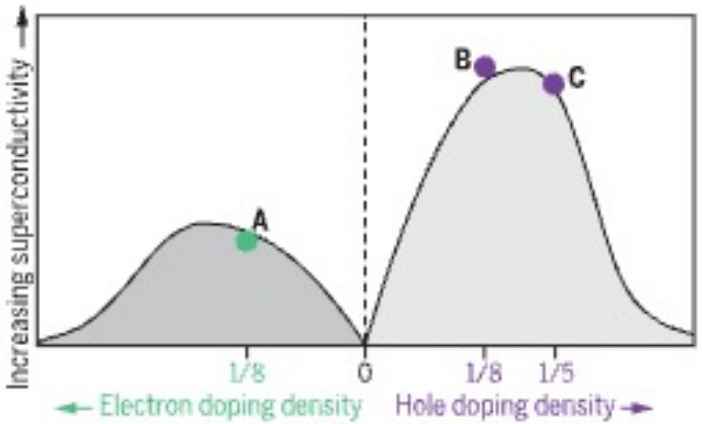

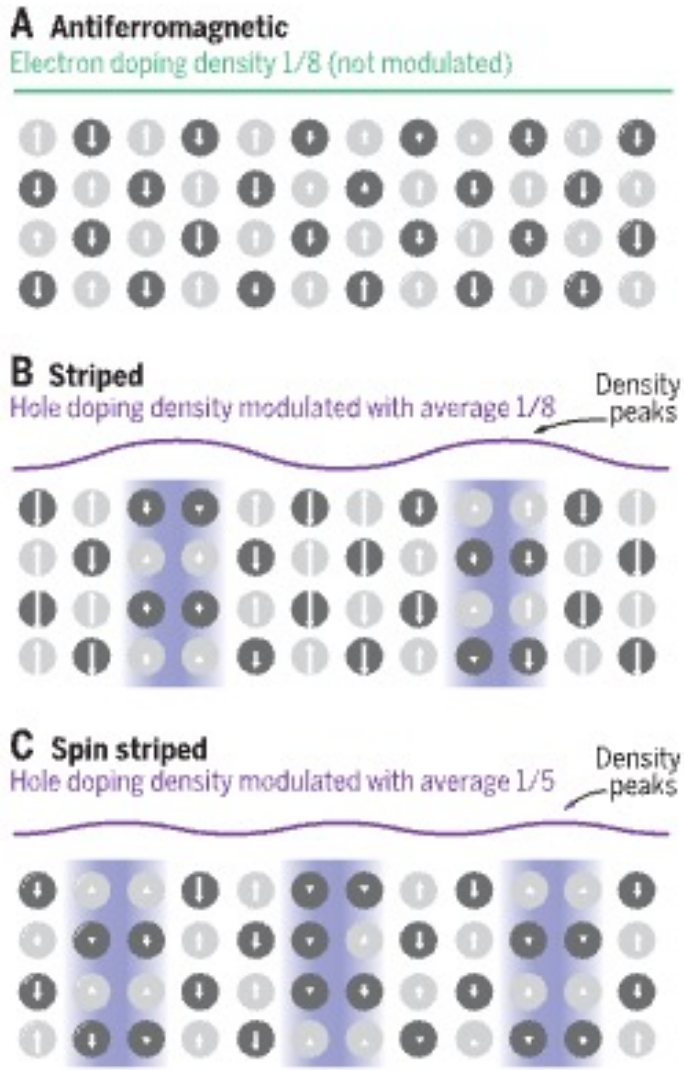

Simple electronic models now reproduce superconductivity

The **Hubbard model** is the standard "minimal" model to capture strong electronic correlations on a lattice:
•electrons live on a square lattice (like Cu sites)
•they can **hop** to neighboring sites with amplitude *t*
•if two electrons land on the same site, they pay a large energy penalty *U* (strong on-site repulsion)

At **half-filling** (one electron per site), and for large *U*, the Hubbard model naturally gives a **Mott insulating antiferromagnet**, just like undoped cuprates.

Homework:
12.2-12.6
12.11 – 12.14